GEO-SEQ Project
Status and Cost Report
June 1–September 30, 2003 Period

Project Overview

The purpose of the GEO-SEQ Project is to establish a public-private R&D partnership that will:

➢ Lower the cost of geologic sequestration by: (1) developing innovative optimization methods for sequestration technologies with collateral economic benefits, such as enhanced oil recovery (EOR), enhanced gas recovery (EGR), and enhanced coalbed methane production; and (2) understanding and optimizing trade-offs between CO_2 separation and capture costs, compression and transportation costs, and geologic sequestration alternatives.

➢ Lower the risk of geologic sequestration by: (1) providing the information needed to select sites for safe and effective sequestration; (2) increasing confidence in the effectiveness and safety of sequestration by identifying and demonstrating cost-effective monitoring technologies; and (3) improving performance-assessment methods to predict and verify that long-term sequestration practices are safe, effective, and do not introduce any unintended environmental impact.

➢ Decrease the time to implementation by: (1) pursuing early opportunities for pilot tests with our private-sector partners and (2) gaining public acceptance.

In May 2000, a project kickoff meeting was held at Ernest Orlando Lawrence Berkeley National Laboratory (Berkeley Lab) to plan the technical work to be carried out, starting with FY00 funding allocations. Since then, work has been performed on four tasks: (A) development of sequestration co-optimization methods for EOR, depleted gas reservoirs, and brine formations; (B) evaluation and demonstration of monitoring technologies for verification, optimization, and safety; (C) enhancement and comparison of computer-simulation models for predicting, assessing, and optimizing geologic sequestration in brine, oil, and gas, as well as coalbed methane formations; and (D) improvement of the methodology and information available for capacity assessment of sequestration sites. Recently, a new task in support of the Frio Brine Pilot Project (E) has been added.

This Reporting Period's Highlights

➢ Most GEO-SEQ team efforts were directed towards the Frio Brine Pilot project (Task E).

➢ Field and laboratory plans for baseline data acquisition, fluid sampling and analysis, well testing, and geophysical monitoring activities for the Frio test are near completion.

➢ Remotely controlled electrical-resistance tomography data acquisition was successfully tested and deployed in the field.

➢ GEO-SEQ team investigators continued to model the evolution of an injected CO_2 plume, assuming different well activities and reservoir properties.

Papers Presented, Submitted, Accepted, or Published during This Period

Cakici, M.D. and A.R. Kovscek, Geologic storage of carbon dioxide and enhanced oil recovery II: Cooptimization of storage and recovery. Paper to be submitted to Energy Conversion and Management, 2003.

Doughty, C., TOUGH2 simulations of the Frio Pilot CO_2 injection test. Talk presented at Berkeley Lab's Earth Sciences Division Town Hall Meeting, June 2003.

Hoversten, G.M., R. Gritto, J. Washbourne, and T.M. Daley, Pressure and fluid saturation prediction in a multicomponent reservoir, using combined seismic and electromagnetic imaging. *Geophysics*, **68**, pp. 1580–1591; Berkeley Lab Report # LNBL-51281, 2003.

Hovorka, S.D., C. Doughty, S.M. Benson, S. M., K. Pruess, and P.R. Knox. Assessment of the impact of geological heterogeneity on CO_2 storage in brine formations: A case study from the Texas Gulf Coast. In: Geological Storage for Emissions Reduction: Technology (S.J. Baines, J. Gale, and R.H. Worden, eds.), Geological Society (London) Special Publication (in press), Berkeley Lab Report # LNBL-51390, 2003.

Jessen, K., A.R. Kovscek, and F.M. Orr, Jr., Increasing CO_2 storage in oil recovery. Paper submitted to *Energy Conversion and Management*, 2003.

Law, D.H.-S., and W.D. (Bill) Gunter, History matching of enhanced coalbed methane (ECBM) Production Field Data. Paper presented at the 2nd International Workshop on Research Relevant to CO_2 Sequestration in Coal Seam, Tokyo, Japan, September 25, 2003,.

Oldenburg, C.M., S.H. Stevens, and S.M. Benson, Economic feasibility of carbon sequestration with enhanced gas recovery (CSEGR). *Energy,* 2004 (in press.

Oldenburg, C.M., S.W. Webb, K. Pruess, and G.J. Moridis, Mixing of stably stratified gases in subsurface reservoirs: A comparison of diffusion models. *Transport in Porous Media*, **54**(3), pp. 323–334, 2004; Berkeley Lab Report # LBNL-51545.

Pruess, K., J. García, T. Kovscek, C. Oldenburg, J. Rutqvist, C. Steefel, and T. Xu, Code intercomparison builds confidence in numerical simulation models for geologic disposal of CO_2. *Energy Conversion and Management*, 2003 (in press); Berkeley Lab Report # LBNL-52211.

Wang, Y and A.R. Kovscek, Geologic storage of carbon dioxide and enhanced oil recovery I: Uncertainty quantification employing a streamline-based proxy for reservoir flow simulation. Paper to be submitted to *Energy Conversion and Management*, 2003.

Zhu, J., K. Jessen, A. R. Kovscek, and F.M. Orr, Jr., Analytical Solutions for Coal-Bed Methane Displacement by Gas Injection. Society of Petroleum Engineers Journal, 8 (4), pp. 371-379, 2003.

Task Summaries

Task A: Develop Sequestration Co-Optimization Methods

Subtask A-1:   Co-Optimization of Carbon Sequestration, EOR, and EGR from Oil Reservoirs

Goals

To assess the possibilities for co-optimization of CO_2 sequestration and enhanced oil recovery (EOR), and to develop techniques for selecting the optimum gas composition for injection. Results will lay the groundwork necessary for rapidly evaluating the performance of candidate sequestration sites, as well as monitoring the performance of CO_2 EOR.

Previous Main Achievements

➢ Screening criteria have been generated for selection of oil reservoirs that would co-optimize EOR and maximize CO_2 storage in a reservoir.
➢ A streamline-based proxy for full reservoir simulation has been thoroughly studied. It allows rapid selection of a representative subset of stochastically generated reservoir models that encompass uncertainty with respect to true reservoir geology.

➢ Reservoir simulation studies of co-optimization have shown that storage of CO_2 can be increased, with little or no loss in oil production, through active control of injection and production conditions while injecting pure CO_2.

Accomplishments This Period

We determined that producing gas-oil ratio (GOR) and injection pressures are two robust, easily measurable parameters, both to use as control parameters in a well-control scheme that limits gas produced by the wells, and to increase gas contact with reservoir volume.

Progress This Period

Previously, a synthetic, three-dimensional, heterogeneous, stochastic model of an oil reservoir was used to simulate various reservoir development scenarios. These simulations delineated techniques that simultaneously optimize the volume of oil produced and the mass of CO_2 stored in the reservoir. Injection gases included both pure CO_2 that is immiscible in a 15-component, moderately heavy crude oil (24°API) and a solvent gas composed of 2/3 CO_2 (with the remaining injected gas being rich hydrocarbon gases). It was shown that a conventional water-alternating gas (WAG) oil recovery scheme is to some degree counter to the goals of co-optimization. Substantial reservoir pore volume is filled with water during WAG that could otherwise be filled with CO_2. A process of well control in which production wells are actively monitored and controlled limits the amount of produced gas and increases the contact of gas with reservoir volume. The well-control technique recovers at least as much oil as the conventional WAG technique, while storing more than 2.5 times as much CO_2.

Work during this period showed that the producing gas-oil ratio (GOR) and the injection pressure are robust parameters to use for well control. They are easily measured and give the desired results. Moreover, the control scheme is easily tuned using these parameters, and control is robust. Other parameter sets were tested, but did not perform as well as producing GOR and injection well pressure. The control strategy was extended to individual segments of the well, as opposed to controlling an entire well. The central idea was that a portion of the well might be responsible for a large fraction of gas production, while other segments produced sufficient oil to warrant continued production. Results with this segmented-well-control strategy were only marginally better than our other attempts at well control. Moreover, control was not as robust. All wells in the synthetic model were vertical, and perhaps the segmented well control performs better with horizontal wells. However, this application will remain untested until additional studies are performed (the project is over and funds are all expended).

Additionally, our co-optimization results were written up for journal submission during this period. There are two papers. The first focuses upon quantifying uncertainty, as it relates to CO_2 sequestration, in stochastic reservoir descriptions. In such descriptions, multiple equiprobable models of reservoir-heterogeneity distribution are created, and comprehensive simulation on all models is computationally prohibitive. The paper describes a technique for selecting a small, representative subset of reservoir models for thorough investigation. The second paper details the co-optimization exercise and the development of the well-control strategy summarized above. Both manuscripts are in draft form and should be submitted to *Energy Conversion and Management* by the end of December. A few details remain, such as thorough proofreading and incorporating a grid-sensitivity exercise demonstrating that the simulation grid is fine enough to minimize the effects of numerical dispersion.

A manuscript entitled "Analytical theory of coalbed methane recovery by gas injection" was accepted for publication in the *Society of Petroleum Engineers Journal*. It will appear in the December 2003 issue.

Subtask A-2:   Feasibility Assessment of Carbon Sequestration with Enhanced Gas Recovery (CSEGR) in Depleted Gas Reservoirs

Goals

To assess the feasibility of injecting CO_2 into depleted natural gas reservoirs for sequestering carbon dioxide (CO_2) and enhancing methane (CH_4) recovery. Investigation will include assessments of (1) CO_2 and CH_4 flow and transport processes, (2) injection strategies that retard mixing, (3) novel approaches to inhibit mixing, and (4) identification of candidate sites for a pilot study.

Previous Main Achievements

On the basis of numerical simulation studies, the proof-of-concept for CO_2 storage with enhanced gas recovery (CSEGR) was demonstrated and the economic feasibility of these projects was evaluated

It was found that transport in a high-permeability gas reservoir could be adequately simulated using the Advective Diffusive Model (ADM), but that the Dusty Gas Model (DGM) is more appropriate for lower permeability units.

Accomplishments This Period

➢   The newly developed solubility model was tested and verified.
➢   We initiated planning of the Frio near-surface CO_2 monitoring and modeling project (Task E).
➢   We helped organize and support the Frio pre-injection well and tracer testing (Task E).

Progress This Period

We have been testing and verifying a new solubility model to extend the range of applicability for our TOUGH2/EOS7C code, now used for CSEGR and CO2 cushion-gas simulations. The new code also accurately handles nonisothermal effects and shows accurate results for real-gas mixture enthalpies. The use of real water properties is needed for water-vapor-rich mixtures, because the Peng-Robinson model does not appear to be accurate for superheated steam.

A team was assembled to carry out baseline surface monitoring for the Frio CO2 injection test. This team will do eddy correlation (EC) and accumulation chamber (AC) flux monitoring, as well as gas sampling and analyses. In addition to surface monitoring, we will be modeling with the Land Surface Model (LSM) to build predictive capabilities for the site.

We continued to help a visiting scientist, Dr. Dorothee Rebscher, run simulations of CSEGR for the Salzwedel-Peckenson gas reservoir in eastern Germany.

During this period, two proposals were prepared: (1) on the use of CO_2 as a cushion gas at a large gas storage field near Dallas (Worsham-Steed), and (2) on an innovative air-injection enhanced gas recovery (EGR) and wind farm compressed-air-energy-storage (CAES) project.

Work Next Quarter

➢   •Plan and schedule Frio surface monitoring work.
➢   •Plan and schedule LSM modeling work to accompany the Frio monitoring.
➢   •Continue working with Dr. Rebscher to carry out CSEGR simulations.
➢   •Continue to support the Frio pre-injection testing effort.

Subtask A-3: Evaluation of the Impact of CO_2 Aqueous Fluid and Reservoir Rock Interactions on the Geologic Sequestration of CO_2, with Special Emphasis on Economic Implications.

Goals

To evaluate the impact on geologic sequestration of injecting an impure CO_2 waste stream into the storage formation. By reducing the costs of front-end processes, the overall costs of sequestration could be dramatically lowered. One approach is to sequester impure CO_2 waste streams that are less expensive or require less energy than separating pure CO_2 from the flue gas.

Previous Main Achievements

➢ Potential reaction products have been determined, based upon reaction-progress chemical thermodynamic/kinetic calculations for typical sandstone and carbonate reservoirs into which an impure CO_2 waste stream is injected.
➢ Reactive transport simulations have been completed for a plug-flow reactor (PFR) run using the Frio Formation core material acquired in support of Task E. Additional simulations were performed as part of the Frio Brine Pilot Project planning efforts (Task E).
➢ The PFR was upgraded by installing new pump-operating software.

Accomplishments This Period

➢ During this period, we continued to process the results of a reactive transport experiment intended to validate our reactive transport simulators and to aid in the design of the Frio Pilot Project.
➢ We are working with other GEO-SEQ team members to define the sampling and analysis plan for geochemistry work to be done at the Frio Pilot. This is critical to obtaining the data required for reactive transport modeling and performance assessment at Frio.

Progress This Period

We continued to re-orient our work to more directly support the planning and execution of the Frio Pilot Project, being run in conjunction with the Texas Bureau of Economic Geology (BEG). In FY04, all our effort in this task will be directed towards the Frio Pilot Project. We discussed geochemical sampling needs and potential sampling and analytical protocols with the other GEO-SEQ team members, who will also be involved in field geochemical-sample acquisition and analysis. With BEG and Sandia Technologies personnel, we discussed laboratory pre-pilot tests designed to evaluate the impact of CO_2 on grouts and cements to be used in the injection well. This is required to ensure well-seal integrity during the injection of CO_2, given that it produces quite low-pH, aggressive solutions.

Unfortunately, we must rely on geochemical models (reactive transport simulators) to predict the long-term performance of CO_2 sequestration with respect to caprock and well-bore-seal integrity, given the relatively low kinetic rates of geochemical reactions at reservoir conditions. We *cannot* rely on the Frio Pilot project field experiment or laboratory experiments alone to assess performance. Validating our reactive transport simulators is a critical requirement, because of the long time period over which containment must be assured. Our prior experience benchmarking reactive transport simulators against ideal reactive transport experiments (e.g., Johnson et al., 1998) suggests that our simulators handle dissolution of the more common rock-forming minerals reasonably well. Dissolution processes will dominate the chemical signal seen during the lifetime of the Frio Pilot Project. However, these simulators have not been rigorously evaluated in terms of accurately modeling mineral growth or the geochemical behavior of cement minerals. This is a serious shortcoming that we intend to address.

We have specifically made acquisition of pre-test caprock core, Frio "B" and "C" sands, cement from the injection well, and native groundwater a part of the Frio Pilot sampling program. These samples will allow us to do the lab testing required to properly design the reactive-transport geochemical models. These models will then be used to make a priori calculations of system behavior that may be checked against field results, validating the simulator for those processes occurring on the time scale of the Frio Pilot Project. Longer-term geochemical processes, like mineral growth, will require lab experiments for simulator validation.

As reported last quarter, we completed the first of a planned series of plug-flow reactor (PFR) experiments specifically designed to address this problem. We used a simulator (CRUNCH) to design an experiment that should produce a measurable amount of a clay mineral (kaolinite) reaction product under conditions directly relevant to geologic sequestration of CO_2. This issue is of some practical importance, because in the acidic conditions near the CO_2 injection well, the dissolution of silicate minerals could result in the growth of clay minerals that could decrease injectivity.

Our comparison of predicted (via reactive transport simulation) and actual experimental results of fluid composition evolution with time showed that good agreement was obtained only if silica and aluminosilicate mineral precipitation were suppressed. This suggests that the simulator is not accurately predicting mineral growth, but as of last quarter, the absence of mineral growth in the experiment remained to be verified by analyses of the solid phase. During this reporting period, we continued analyses of the solid phase, including SEM imaging and XRD analyses.

We present (in **Figures 1 and 2)** SEM photos of Frio sand recovered from the experiment that show evidence of reservoir mineral dissolution having occurred. Whether these features are a consequence of the acidic conditions produced by the dissolved CO_2 in the experiment, or are already present, will be addressed below.
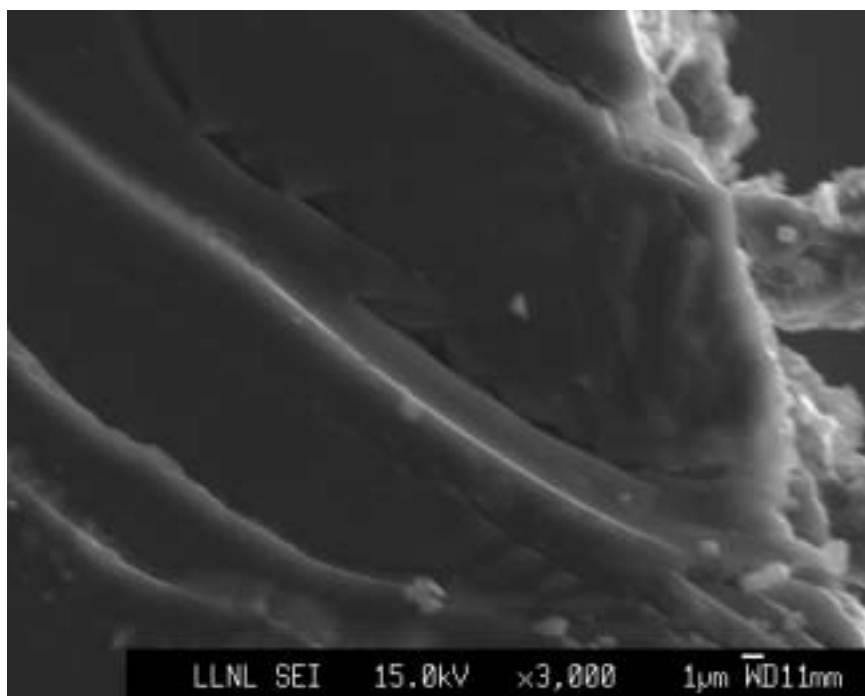

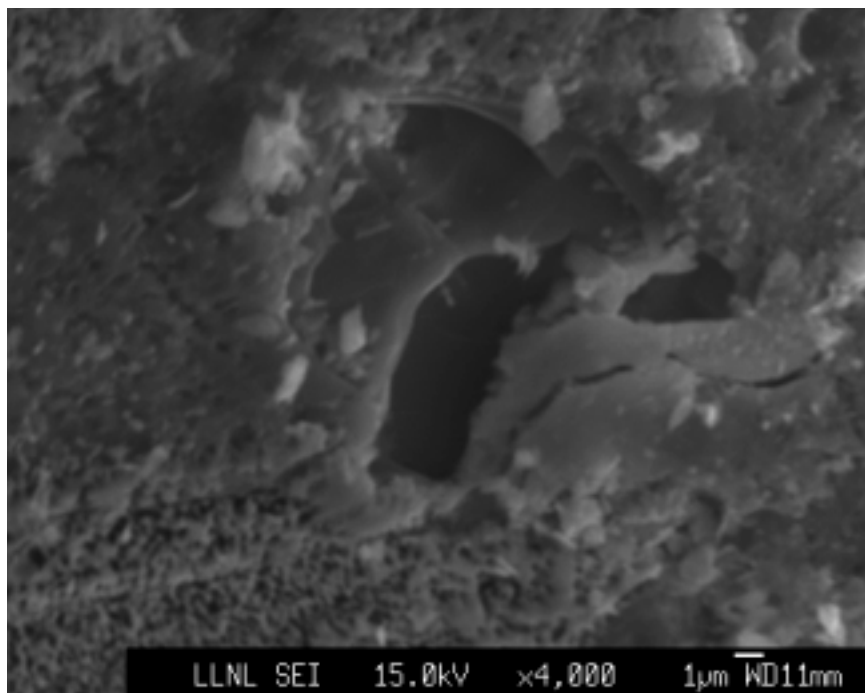**Figure 1.** Etch pits on K-feldspar

Figure 2. Etch pits on K-feldspar and pitting of overlying silica cement

In **Figure 3** we show that many of the mineral grains are at least partially covered by secondary minerals. Again, the key question is whether these minerals were present prior to the run.
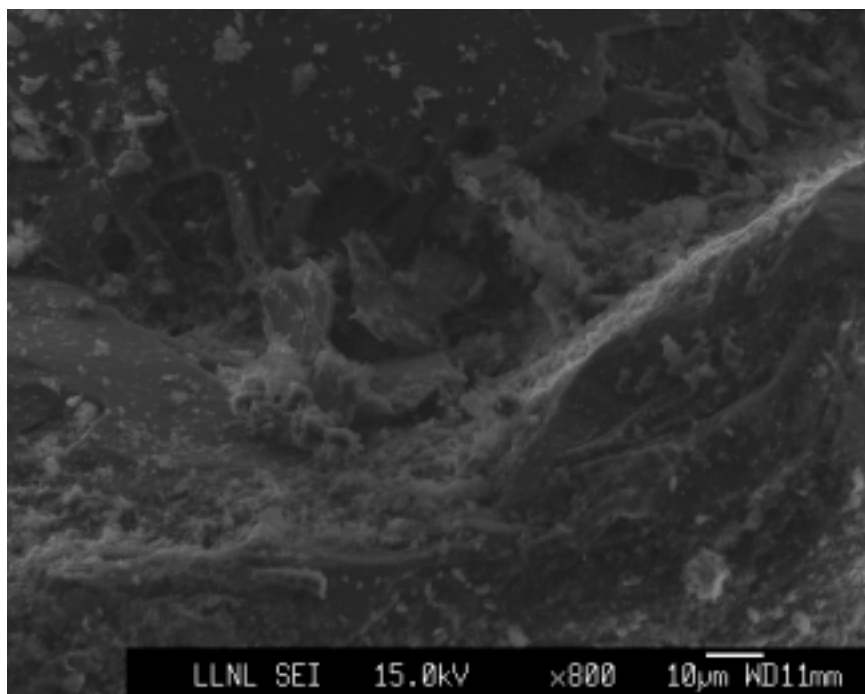

Figure 3. Secondary minerals coating mineral grains

In **Figures 4 and 5** we show unreacted K-feldspar grains from the Frio sand, sieved and ultrasonically washed in methanol, that were the starting material for the experiment. These grains show that the reservoir K-feldspar grains are already etched to some extent, so the etch pits seen on the K-feldspar are not good indicators of dissolution processes that may have occurred during the experiment.
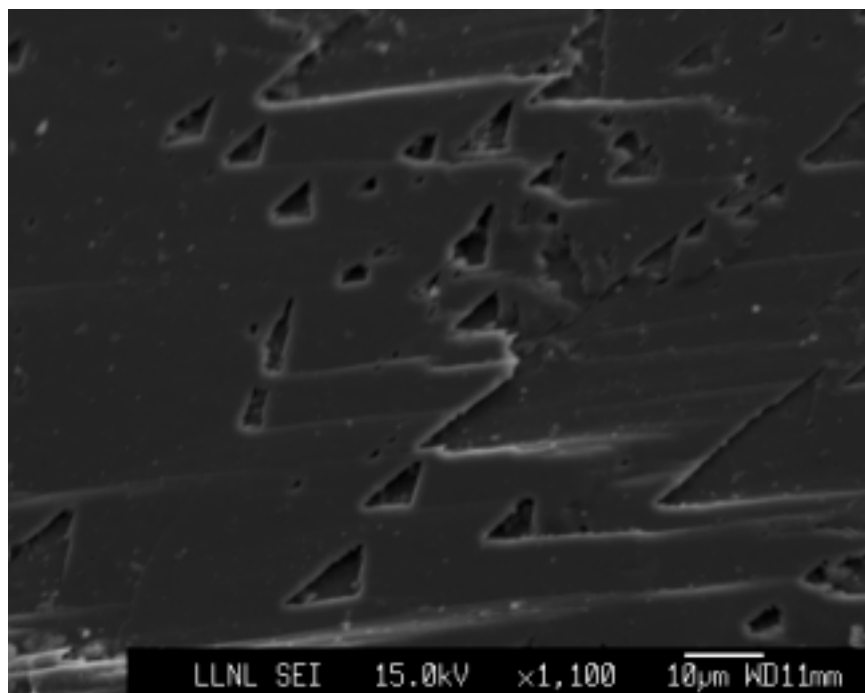
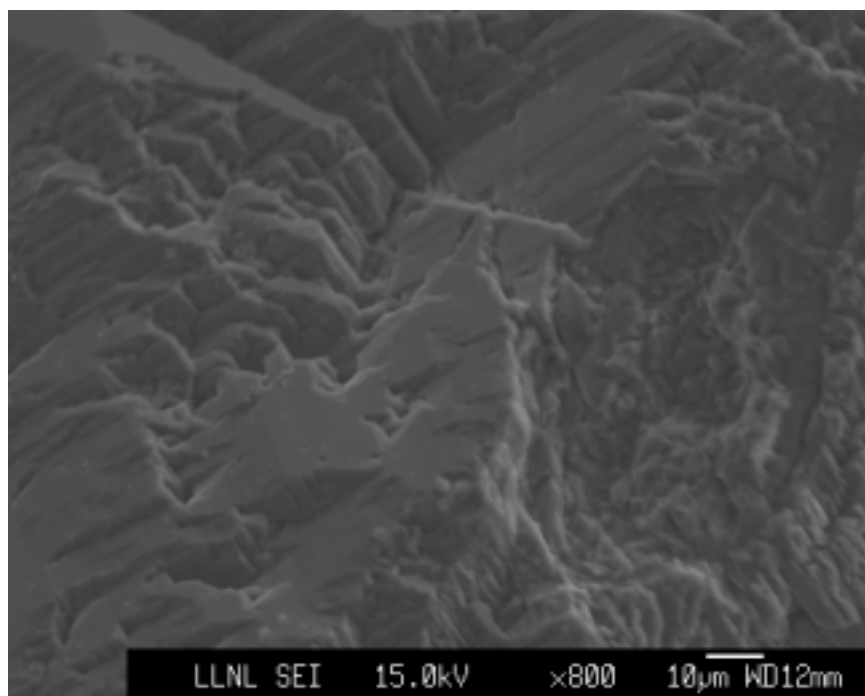**Figure 4.** Etch pits on unreacted K-feldspar grain

Figure 5. Etching of unreacted K-feldspar grain

Notice that the unreacted grains are not covered with secondary mineral grains to the same extent as the run products from the experiment. This suggests that at least some new secondary minerals formed as a result of reaction with the CO_2-rich brine.

We are currently analyzing the reacted grains for mineral changes detectable using XRD, as a function of distribution in space along the core. We will be able to identify and at least semi-quantitatively determine

the production rate of the secondary minerals. This work will be completed within the first few weeks of the new fiscal year (FY04) and be useful for planning purposes in the Frio Pilot Project.

In summary, although the fluid-chemistry results from the experiment show that the reactive transport model overpredicted the production of secondary minerals, analyses of the run products should provide us with the data needed to modify our model input parameters to better match results. In that way, we can produce a reactive transport model that is validated and directly useful in simulating conditions at Frio.

Unfortunately, we need to make model predictions to evaluate any specific site's prospects (a performance assessment exercise) over the long term. This modeling is also needed to correctly assign "credits" for companies doing the sequestering (they will not wait 10 years to get paid). This performance assessment process will be critical in selling the safety of the injection process and the long-term (ultimately hundreds to thousands of years) safety of geologic CO_2 sequestration to the general public. We are totally dependent on models for these purposes, and the models are almost entirely without validation of a truly quantitative sort. Our goal is to provide a validated reactive transport simulator that would be useful in doing the required performance assessment.

Work Next Quarter

Our attention will stay focused on work that will help in the design and conduct of the Frio Pilot Project. We plan to complete analysis of the recently completed reactive transport experiment (PFR14) and use the results to benchmark our simulator. To our knowledge, these experiments provide the first really quantifiable tests of any reactive transport simulator that are directly relevant to CO_2 sequestration. Next quarter, we will collaborate with BEG and Sandia Technologies personnel in making or acquiring cement samples appropriate for durability testing to ensure well bore seal integrity. We will also make pre-injection reactive transport simulations, based on the most current physical model available from Berkeley Lab, to predict the results of Frio Pilot CO_2 injection. Specifically, we will begin work on Subtask E1, Activity 3: Performance Prediction, Geochemical Interactions. This activity is described in the current FY04 FWP for GEO-SEQ.

Task B: Evaluate and Demonstrate Monitoring Technologies

Subtask B-1: Sensitivity Modeling and Optimization of Geophysical Monitoring Technologies

Goals

To (1) demonstrate methodologies for, and carry out an assessment of, the effectiveness of candidate geophysical monitoring techniques; (2) provide and demonstrate a methodology for designing an optimum monitoring system; and (3) provide and demonstrate methodologies for interpreting geophysical and reservoir data to obtain high-resolution reservoir images. The Chevron CO_2 pilot at Lost Hills, California, has been used as an initial test case for developing these methodologies.

Note: This subtask was completed earlier in this fiscal year.

Main Achievements

A methodology for site-specific selection of monitoring technologies was established and demonstrated.

Modeling studies based on well logs from the Liberty Field in southern Texas showed that before CO_2 injection, seismic reflection from shale-sand interfaces decreases in amplitude with increasing depth. As CO_2 is injected at shallow depth, reflectivity sharply decreases.

Those numerical studies also indicated that even if a CO_2 wedge were seismically detected because of geometric effects, interpretation of the reflection for fluid properties would be difficult until the horizontal extent of the CO_2 zone exceeds one seismic Fresnel zone.

Results of other modeling work suggested that injection of CO_2 into the Liberty Field formation would produce an easily measurable streaming potential (SP) response.

Subtask B-2: Field Data Acquisition for CO$_2$ Monitoring Using Geophysical Methods

Goals

To demonstrate (through field testing) the applicability of single-well, crosswell, surface-to-borehole seismic, crosswell electromagnetic (EM), and electrical-resistance tomography (ERT) methods for subsurface imaging of CO$_2$.

Previous Main Achievements

➢ The first test of the joint application of crosswell seismic and crosswell electromagnetic measurements for monitoring injected CO$_2$ was completed.
➢ A scoping study of tiltmeter methods to detect and monitor CO$_2$ injection as part of the Frio Brine Pilot Project (Task E) was refined.
➢ A time-lapse electrical resistance tomography (ERT) casing survey was completed in the Vacuum Field, New Mexico, a CO$_2$ injection site.

Accomplishments This Period

A remotely controlled ERT data acquisition system capable of obtaining full time-lapse data sets on command was tested and deployed in the field. This work was funded separately. The successful deployment will enable frequent surveys for monitoring changes in the field caused by CO$_2$ injection.

Progress This Period

Electrical Resistance Tomography

The field deployment in early September 2003 was used to repair equipment damaged in a lightning storm and collect a time-lapse survey. The data processing for that deployment is complete. This processed data adds another time increment to the monitoring program at the site.

The remotely controlled ERT data acquisition system was operational except for interruptions due to lightning storms in the area. One storm damaged a transformer on a power line feeding our system; this required a shut-down of the remote system in September.

The entire data acquisition system was removed from the ChevronTexaco field site in preparation for deployment to a new site. All data has been processed, and results submitted in the September 2003 final report. Some of the key points are summarized here:

In the course of this work, we refined and partially demonstrated casing ERT for monitoring the sequestration of CO$_2$ in a deep geologic repository. The method has been tested at two different secondary oil recovery sites: a steam flood and a CO$_2$ flood. Owing to operational conditions, confirmation of the interpreted results depends on inference at present. As CO$_2$ injection continues in the field, it is likely that its presence will be detected; however, insufficient volumes were injected in the original survey pattern to be detected, and we are only now able to collect data of sufficient quality over the expanded survey area to process time-lapse surveys where significant changes caused by the presence of CO$_2$ are anticipated. However, the time-lapse surveys show changes consistent with operational changes across the survey areas and with independent measurements (i.e., production records).

The method yields low-resolution tomographs of lateral fluid movement, with no disruption to normal operations. While higher resolution is desirable, this method has some important advantages. First, no new infrastructure (e.g., monitoring well) is required. Second, because there are no moving sensors (e.g., sondes as in crosswell tomography), long-electrode ERT is easily automated and has even been controlled remotely using a satellite communications link. This makes practical on-demand, real-time monitoring, requiring minimal deployment of field personnel. An added benefit is that even though existing well casings are used as electrodes, there is no interruption to normal field operations—the wells can continue to produce or inject while being used to monitor the field. These factors are particularly

appealing for applications in which other operations are occurring; such as in CO_2 enhanced oil recovery. This method complements other higher resolution methods. Changes detected using a low-resolution method such as this one can be investigated through deployment of a higher resolution method. The advantage here is that the more costly high-resolution survey can be focused on the region of interest, rather than be used as an overall survey method.

An abstract ("Electrical Resistance Tomography (ERT) To Image CO_2 Sequestration: Field Trials") has been submitted for presentation at the Fall American Geophysical Union Meeting in San Francisco, December 2003.

Tiltmeters

Simple 3D deformation modeling of the Berkeley Lab flow simulations of the Frio Pilot injection indicate that downhole tilt monitoring—using a vertical string in well SGH3, about 130 m SE of the planned injection well—could be used to map the vertical and lateral extents of the CO_2 plume (at least in the SE quadrant). We have received a very competitive cost proposal to perform continuous downhole monitoring using a 12-tool vertical array over the 5-day period envisioned for the experiment. We have also received preliminary cost estimates for reentering well SGH3.

Work Next Quarter

Electrical Resistance Tomography

We have processed and analyzed time-lapse surveys to monitor changes in the field during CO_2 injection. Interpretation included comparison to operations and independent reservoir data. This material is reported in the final project report submitted in September 2003. At present, electrical imaging is not planned for the Frio Pilot.

Tiltmeters

Our primary objective in the first quarter of FY04 is to carry out tilt monitoring of the Frio Pilot. Meeting this objective will depend on whether the funding allocation is sufficient to meet the costs of the tilt monitoring and well reentry, and whether funding is received sufficiently in advance of the pilot experiment to enable the subcontracts to be let. Once this has been determined, we will revise plans and design for a tiltmeter survey as part of the Frio Pilot to reflect the new funding level.

Major Difficulties and Planned Corrective Actions

Electrical Resistance Tomography

The major ERT difficulty was caused by severe lightning storms at the site in the late summer of 2003. These storms produced high winds and lightning-induced electrical surges in our measurement lines, as well as in our utility power cables. The high winds pushed the parabolic antenna for the satellite link enough to interrupt the link. However, this interruption was only temporary, and we could reestablish the link after the storms. The electrical surges burned out fuses in some equipment and burned traces off IC boards in other equipment. This was not a temporary interruption; it required a trip to the site to repair the damage. Electrical surges in the utility power actually destroyed a power pole transformer, requiring our system to be shut down until the power company repaired the damage. The corrective action is to keep the measurement system disconnected from utility power and from all the wellheads except during data acquisition, which will be accomplished only during good weather conditions. No further corrective action is required.

We tested and deployed a remotely controlled ERT data acquisition system in the field, one that is capable of obtaining full time-lapse data sets on command. Successful deployment of this system will enable frequent surveys for monitoring changes in the field caused by CO_2 injection.

Subtask B-3: Application of Natural and Introduced Tracers for Optimizing Value-Added Sequestration Technologies

Goals

To provide methods that utilize the power of natural and introduced tracers to decipher the fate and transport of CO_2 injected into the subsurface. The resulting data will be used to calibrate and validate predictive models utilized for (1) estimating CO_2 residence time, reservoir storage capacity, and storage mechanisms; (2) testing injection scenarios for process optimization; and (3) assessing the potential leakage of CO_2 from the reservoir.

Previous Main Achievements

➢ Laboratory isotopic-partitioning experiments and mass-balance isotopic-reaction calculations have been done to assess carbon- and oxygen-isotope changes (focused on the influence of sorption) as CO_2 reacts with potential reservoir phases.
➢ Detailed experiments have been conducted on perfluorocarbon tracer gas-chromatography analytical methods, reproducibility, and sensitivity as a prelude to tracer flow experiments.
➢ Gas and isotope compositions indicate a slight dilution of injected CO_2 by indigenous reservoir gas in selected wells at the Lost Hills, California site.

Progress This Period

Starting in June, the GEO-SEQ efforts of the ORNL team focused on Subtask B-3A (Frio-related activities)

Subtask B-3A: The Frio Pilot Test Monitoring with Introduced Tracers and Stable Isotopes

Goals

To provide tracer and stable isotope methods that will help quantify the fate and transport of CO_2 injected into the subsurface at the Frio, Texas, site (Task E). The resulting data will be used to calibrate and validate predictive models used for (1) estimating CO_2 residence time, reservoir storage capacity, and storage mechanisms; (2) testing injection scenarios for process optimization; and (3) assessing the potential leakage of CO_2 from the reservoir.

Previous Main Achievements

➢ Gas chemistry and isotope analyses of CO_2 from the BP Hydrogen 1 plant, Texas City, Texas, were conducted in support of permitting documentation needed to inject CO_2 into the Frio formation (Task E).
➢ Preliminary mineralogical characterization of the Frio Formation sandstone sample was completed.

Accomplishments This Period

➢ Adsorption and desorption isotherms of CO_2 in Frio sandstone were measured at elevated temperatures and pressures relevant for the planned injection test.
➢ A more comprehensive sampling and analysis plan for the Frio CO_2 injection test was prepared in coordination with investigators at Berkeley Lab, LLNL, Alberta Research Council, USGS, and BEG.

Progress This Period

High-Temperature, High-Pressure CO_2 Sorption in Frio Sandstone

During this period, we determined the adsorption and desorption isotherms for CO_2 in Frio sandstone (Felix Jackson #62, Oyster Bayon Field, Chambers Co., TX, sample provided by Paul Know of Texas Bureau of Economic Geology [BEG]). The purpose of this activity was two fold: (1) to assess the nature of

the interaction between the CO_2 and Frio sand, and (2) to quantify, to the extent possible, the sorptive capacity of the sand for CO_2. A specially constructed high-temperature, high-pressure sorption apparatus was used to measure CO_2 isotherms in small chips (~0.5 to 0.8 mm in diameter) of Frio sandstone at 20.84 and 48.59^{o}C from 0 to 20 bars CO_2 pressure. The results of these experiments are shown in **Figures 6 and 7** for 20.84 and 48.59^{o}C, respectively. Regardless of the temperature of interaction, the following trends are observed: a small but measurable increase in CO_2 uptake at very low pressure, followed by a steady increase in the mass of CO_2 lost to the solid, with a small, but noticeable desorption hysteresis loop. Details of the low-pressure uptake were presented previously from measurements made at 0 and 20°C (June–August 2002 Quarterly Report). CO_2 uptake is slightly greater at the higher temperature. The steady increase in CO_2 uptake is suggestive of multilayering of CO_2 onto quartz, feldspar, and clay surfaces that line the pores of the sandstone. The small, rapid increase at low pressure may be indicative of capillary-like filling of the smallest pores. We observed no high-pressure equivalent to this behavior, as is commonly observed with water uptake in porous rocks.
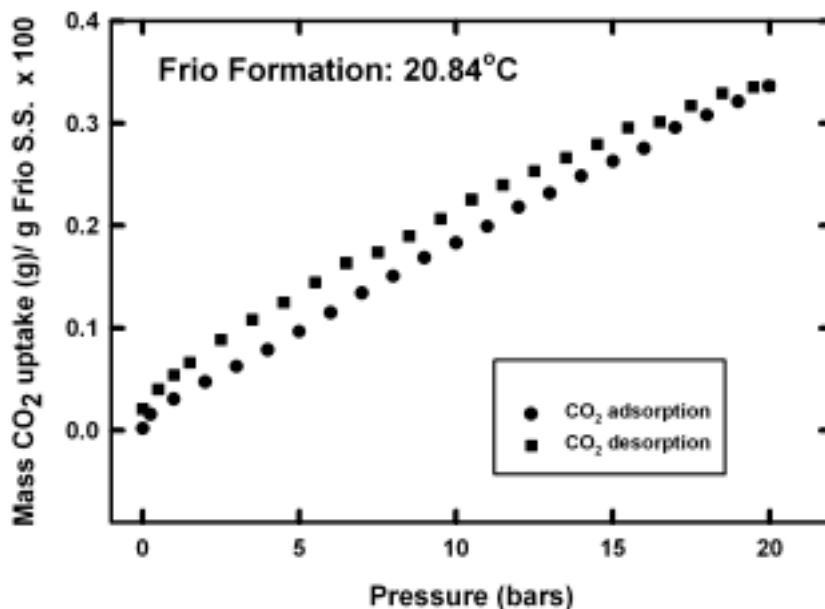

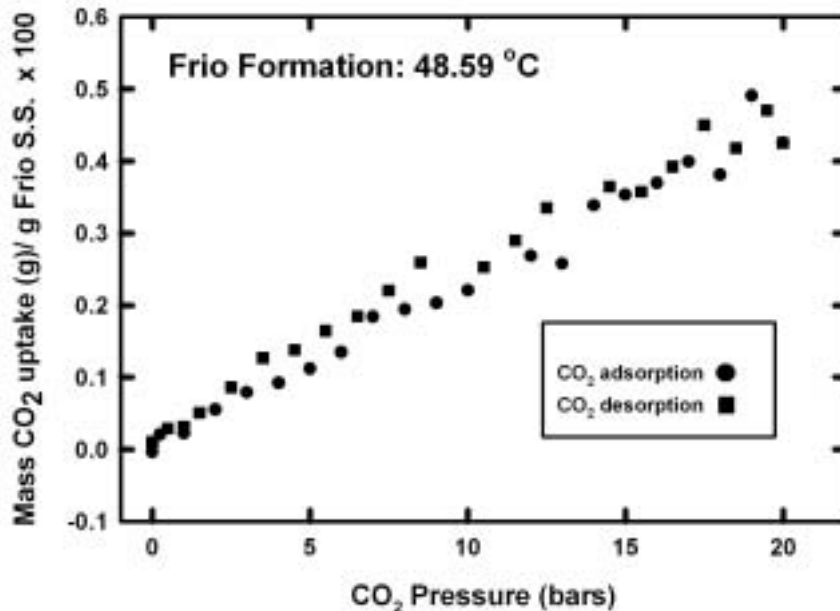**Figure 6.** Sorption isotherms for CO_2 in Frio sandstone determined at 20.84^{o}C.

Figure 7. Sorption isotherms for CO_2 in Frio sandstone determined at 48.59^{o}C.

13

Based on these results, we can extrapolate the sorptive capacity of the Frio for CO_2 to conditions thought to prevail during the Frio Pilot injection test—i.e., ~$50^{o}C$ and CO_2 pressures approaching 150 bars. Assuming that no capillary-like pore filling occurs at pressures above the limit of our experiments (20 bars), we can estimate the amount of CO_2 lost to one gram of sandstone at 150 bar pressure. This value is approximately 0.003g CO_2/g of Frio. For a formation thickness of 80 ft and plume dimensions of 100 × 100 ft, we calculate the mass of rock to be 6×10^{10} g, assuming a density of 2.65 g cc^{-1}. From these two estimates, we calculate that ~200 tons of CO_2 may be lost to the formation just as a result of sorption. This estimate represents a minimum because capillary pore filling could contribute far more to the solid, by mass, than simple sorption. Current plans call for the injection of roughly 3,500 tons of CO_2, of which something like 6% could be retained by the formation.

Our previously reported carbon and oxygen isotope partitioning data indicate that isotopic enrichment occurs in the free gas relative to the gas sorbed onto the solid. The magnitude of this effect varies with the type of substrate and its surface area, and is smaller for carbon than oxygen. Despite only losing roughly 6% by mass of the CO_2 to the solid, we might anticipate an oxygen isotopic shift in the CO_2 of between 0.5 and 1 per mil for the type of quartz-feldspar-clay mineralogy comprising the Frio Pilot. One objective in our assessment of the isotopic composition of CO_2 during the Frio injection test will be to differentiate between behaviors related to sorption and potentially larger oxygen isotope shifts attendant with CO_2 loss to the brine.

Input on Sampling and Analysis for the Frio Injection Test

During this period, input on fluid sampling and analysis was sent to Alan Dutton at BEG for consideration (see Appendix A).

Work Next Quarter

➢ Continue preparation for the Frio CO_2 injection test.
➢ Measure carbon and oxygen isotope partitioning on Frio sandstone chips.

Task C: Enhance and Compare Simulations Models

Subtask C-1: Enhancement of Numerical Simulators for Greenhouse Gas Sequestration in Deep, Unmineable Coal Seams

Goals

To improve simulation models for capacity and performance assessment of CO_2 sequestration in deep, unmineable coal seams.

Previous Main Achievements

➢ Comparisons for Parts I–III with Problem Sets 1–4 have been completed with eight participants from CMG's GEM, CSIRO/TNO's SIMED II, ARI's COMET, GeoQuest's ECLIPSE, BP's GCOMP, Imperial College's METSIM2, Pennsylvania State University's PSU-COALCOMP and Shell's MoReS.
➢ Field data obtained from two single-well micropilot tests with pure CO_2 and flue gas injection conducted by the Alberta Research Council (ARC) at the Fenn Big Valley site, Alberta, Canada, have been released to five participants (TNO, BP, CMG, ARI, and Imperial College) for history matching (i.e., Problem Set 5). History matching provides an opportunity to validate new simulation-model developments in a realistic field situation.
➢ Initial history-matching results from CSIRO/TNO's SIMED II and Imperial College's METSIM2 were collected for the Fenn Big Valley site and were documented.

Main Achievements This Period

➢ History matching of ARC's micro-pilot test data in Part IV has been completed with six participants from CMG's GEM, CSIRO/TNO's SIMED II, ARI's COMET, BP's GCOMP, Imperial College's METSIM2 and Pennsylvania State University's PSU-COALCOMP.

➤ GEO-SEQ Project, 3rd Workshop on "Numerical Modeling of Enhanced Coalbed Methane (ECBM) Recovery" has been held by ARC in Tokyo, Japan, September 26, 2003 to discuss the capability of ECBM numerical models for history matching the ARC's micro-pilot test data.

Progress This Period

History matching of ARC's micropilot test data in Part IV has been completed with six participants from CMG's GEM, CSIRO/TNO's SIMED II, ARI's COMET, BP's GCOMP, Imperial College's METSIM2 and Pennsylvania State University's PSU-COALCOMP. Field data in Part IV has also been released to Shell International, The Netherlands, for history matching using the numerical model, MoReS. However, no history-matching results have been received yet.

Figures 8 and 9 show history-matching results of production gas composition for a single well micropilot test with pure CO_2 injection, using CMG's GEM and ARI's COMET. Production gas composition is the most difficult field data to match. It is believed that a good understanding of the mixed gas sorption and diffusion mechanisms is essential to match these data.
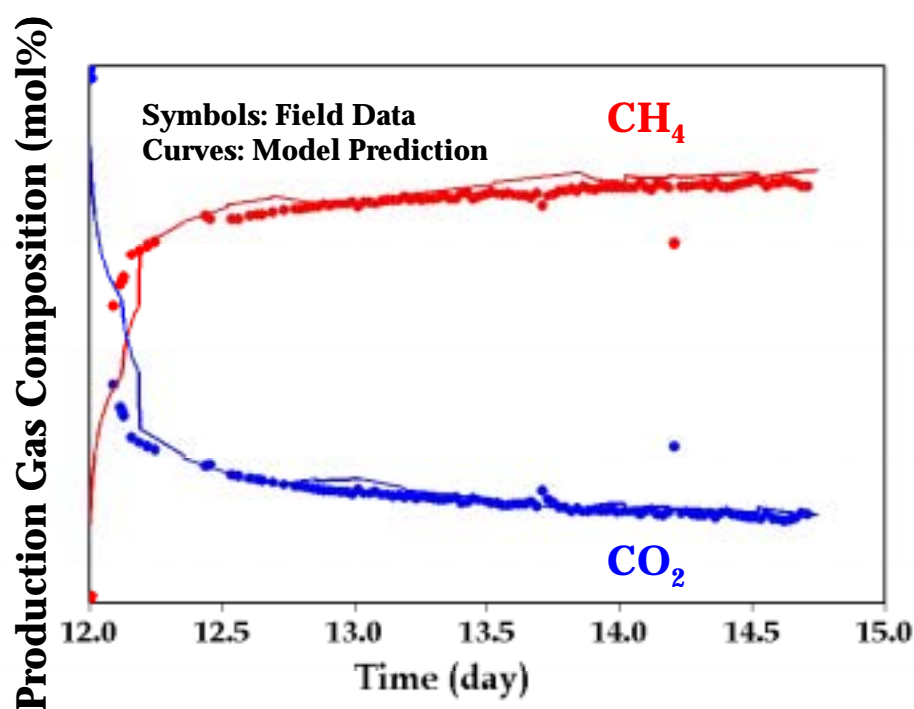
Figure 8: History matching using CMG's GEM
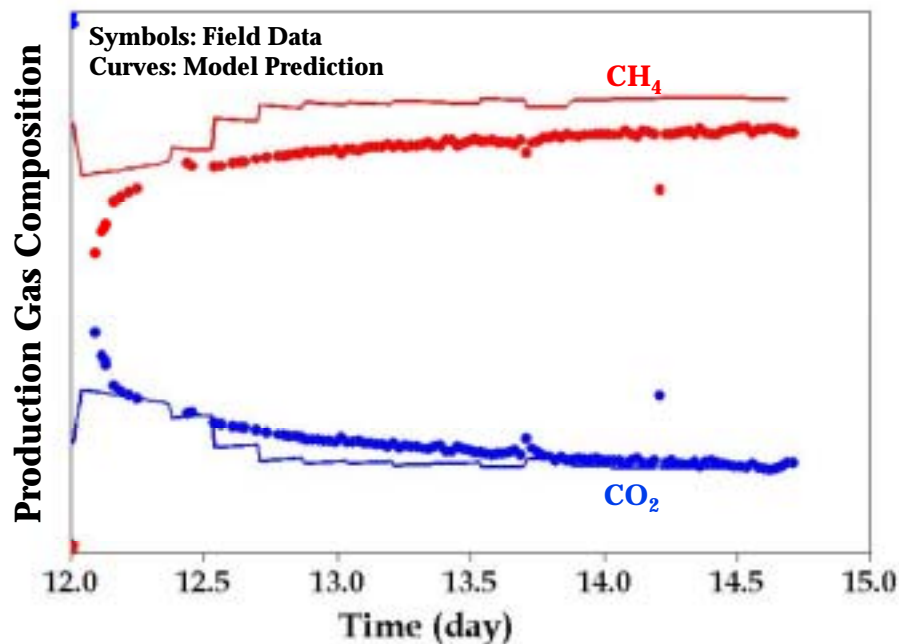
Figure 9: History match using ARI's COMET

GEO-SEQ Project, 3rd Workshop on "Numerical Modeling of Enhanced Coalbed Methane (ECBM) Recovery" was held by ARC in Tokyo, Japan, September 26, 2003. The 19 meeting participants[1] discussed the capability of ECBM numerical models for history matching with the ARC's micropilot test data. Topics addressed included improved history matching through incorporation of special numerical features, to better handle the permeability variation caused by stress and gas sorption and mixed gas diffusion between coal natural fracture system and matrix. Details of this workshop can be found, in the near future, on the ARC's password-protected website: http://www.arc.ab.ca/extranet/ecbm/ (user name: ecbm and password: methane2). This site will offer the presentations given by David Law, Ji-Quan Shi and Turgay Ertekin describing the history match using ECBM models: CMG's GEM, ARI's COMET, Imperial College's METSIM2 and PSU's COALCOMP. A presentation given by Shiji Yamaguchi on "ECBM Modeling in Japan" will also be included.

A paper summarizing all the history-matching results from different numerical models will be submitted for presentation at the Seventh International Conference on Greenhouse Gas Control Technologies (GHGT-7), September 5–9, 2004, Vancouver, British Columbia, Canada.

All comparison results for Subtask C-1 have been updated and will be posted in the near future on the aforementioned ARC's password-protected website.

---

[1]Rob Arts (TNO, The Netherlands), Yuzuru Ashida (Kyoto University, Japan), Andreas Busch (Aachen University, Germany), Turgay Ertekin (Pennsylvania State University, U.S.A.), Brian Evans (Curtin University of Technology, Australia), Masaji Fujioka (Japan Coal Energy Center, Japan), Bill Gunter (ARC, Canada), Kazuo Ishida (Mitsubishi Heavy Industries, Japan), David Law (ARC, Canada), Hong Li (Geoscience Research Laboratory, Japan), Matt Mavor (Tesseract, U.S.A.), Yukihiro Mizuochi (Sumiko Consultants Co. Ltd., Japan), Kotaro Ohga (Hokkaido University, Japan), Kazumi Osato (Geothermal Energy and Research Development Co., Japan), Ji-Quan Shi (Imperial College, U.K.), Sohei Shimada (University of Tokyo, Japan), Ziqiu Xue (RITE, Japan), Shiji Yamaguchi (Akita University, Japan) and Toyohiko Yamazak (Waseda University, Japan).

<u>**Subtask C-2: Intercomparison of Reservoir Simulation Models for Oil, Gas, and Brine Formulations**</u>

Goals

To stimulate the development of models for predicting, optimizing, and verifying CO_2 sequestration in oil, gas, and brine formations. The approach involves: (1) developing a set of benchmark problems; (2) soliciting and obtaining solutions for these problems; (3) holding workshops that involve industrial, academic, and laboratory researchers; and (4) publishing results.

Note: This subtask was completed earlier in this fiscal year.

Main Achievements

➢ A workshop on the code intercomparison project was held at Berkeley Lab on October 29–30, 2001, with the initial modeling results by different groups showing reasonable agreement for most problems.
➢ The final report on the code intercomparison study was issued.
➢ A detailed report that included Berkeley Lab results on the saline aquifer test problems was completed.

Task D: Improve the Methodology and Information for Capacity Assessment

Goals

To improve the methodology and information available for assessing the capacity of oil, gas, brine, and unmineable coal formations, and to provide realistic and quantitative data for construction of computer simulations that will provide more reliable sequestration-capacity estimates.

Previous Main Achievements

➢ A new definition of formation capacity, incorporating intrinsic rock capacity, geometric capacity, formation heterogeneity, and rock porosity, was developed for use in assessing sequestration capacity.
➢ Many modeling studies of the Frio Brine Pilot Experiment (Task E) were completed, assuming different CO_2 injection scenarios and geologic models.
➢ We developed a basin-scale conceptual model of geologic complexity for the Frio Brine Pilot Experiment site (Task E). Quantitative data has been compiled to probabilistically and deterministically create a simulation for the basin.
➢ We extended the modeling studies of the post-injection period for the Frio Brine Pilot Experiment from one year to 100 years. As in previous studies, the choice of characteristic curves has a strong impact on CO_2 plume evolution

Accomplishments This Period

➢ Compared simulations of constant and pulsed pumping at monitoring well during Frio Brine Pilot Test
➢ Included heat flow and temperature changes in CO_2 injection simulation
➢ Began to study the evolution of the CO_2 plume evolution using hysteretic characteristic curves
➢ Developed and applied the Version 0.5 model to simulate CO_2 injection and the rest (nonactivity) period that followed.

Progress This Period

During this period, as in recent quarters, most of the work under this Task focused on Frio-related activities.

Compare Simulations of Constant and Pulsed Pumping at Monitoring Well during Frio Brine Pilot

During the course of the Frio Brine Pilot, we will need to collect samples from the monitoring well. We want to know how producing the monitoring well will impact CO_2 plume evolution and how it will affect the kind of data we can collect. For example, would constant or pulsed production be preferable? To address this question with numerical modeling studies, a new, simplified two-dimensional (2D, i.e., one-layer) model has been developed that has finer lateral grid resolution than the previously used three-dimensional (3D) "Version 0" model.

If the monitoring well is produced in pulses, each pulse must extract at least one wellbore volume of fluid, to get a sample representing formation fluid. Assuming wellbore dimensions of tubing inner diameter $2r_t = 2"$ (0.05 m), tubing length $h_t = 1500$ m, well casing diameter $2r_c = 5.5"$ (0.14 m), casing length $h_c = 66$ m (6 m in "C" sand plus 60 m extension below "C" sand for geophysics), we get

$$V = \pi r_t^2 h_t + \pi r_c^2 h_c = 4,200 \text{ L}$$

Thus, using a pumping rate of 1 L/s (1 kg/s brine), pulse duration should be at least 4,200 s = 1.17 hour.

The following scenarios are considered:

➢ CO_2 injection only (250 T/day (2.9 kg/s) for 15 days)
➢ Injection + small production from monitoring well
        Constant (14.4 T/day = 0.17 kg/s)
        Pulsed (2 hours on at 86.4 T/day (1 kg/s), 10 hours off)
➢ Injection + large production from monitoring well
        Constant (42 T/day = 0.48 kg/s)
        Pulsed (2 hours on at 250 T/day (2.9 kg/s), 10 hours off)

Note that before CO_2 arrives at the monitoring well, brine production at 86.4 or 250 T/day corresponds to 16 or 46 gpm, respectively. The density of the brine/CO_2 mixture is smaller, so the volumetric flow rate is bigger after CO_2 arrival.

Simulation results are summarized in **Figure 10**, which shows the time evolution of pressure P and gas saturation S_g at the injection and monitoring wells for a 15-day CO_2 injection period. There is an earlier CO_2 arrival at the monitoring well and a smaller pressure increase for the larger production rate. The choice of pulsed or constant production does not alter the CO_2 arrival time at the monitoring well, but there is evidence of pulsing for the large production rate. Note that the pressure response at the monitoring well indicates when the front arrives, with the strongest signal provided for the large pulsed production case. The colored dots shown on the time axis identify the times of individual pulses shown in **Figure 11** (discussed below). The shape of the CO_2 plumes for the pulsed and constant production cases (not shown) are nearly indistinguishable from the injection-only case.
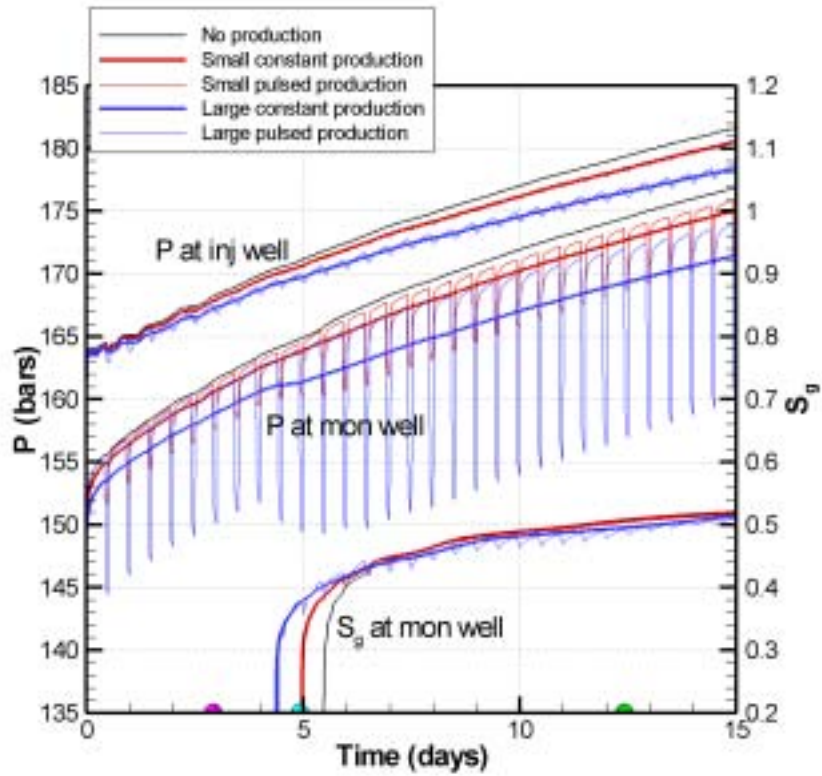
Figure 10. Time evolution of pressure P and gas saturation S_g at the injection and monitoring wells for a 15-day CO_2 injection period, with various assumptions for monitoring well production
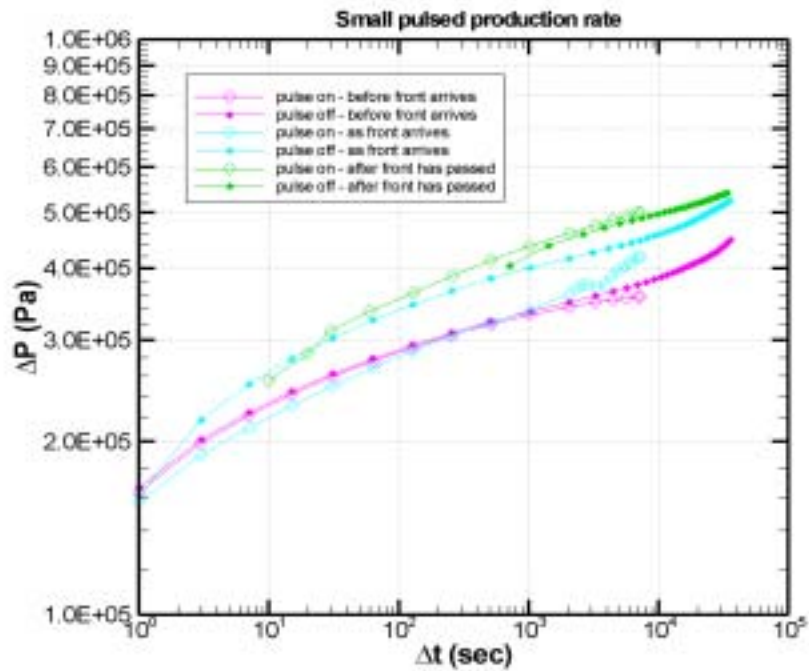

Figure 11. A zoomed-in view of three of the pulse responses for the small production rate. The start time of each pulse is identified by a colored dot in Figure 10.

The phase composition of the fluid produced at the monitoring well is compared to the gas saturation in **Figure 12**, for the large constant and pulsed production rates. The gas-phase fraction of produced fluid (FF_g) does not equal gas saturation S_g. Rather, FF_g is proportional to gas-phase mobility kk_{rg}/μ_g, where k is intrinsic permeability k_{rg} is relative permeability to the gas phase, and μ_g is gas-phase viscosity. For the Corey relative permeability function we use, $k_{rg} = (S_g-S_{gr})^4$, where S_{gr} is residual gas saturation.
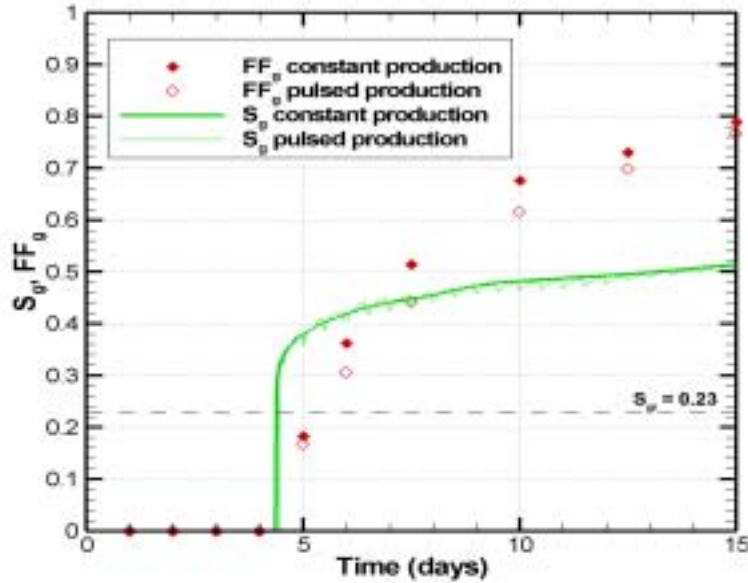
Figure 12. Comparison of the gas-phase fraction of produced fluid (FF_g) and the gas saturation S_g at the monitoring well for constant and pulsed production cases

Figure 11 shows a zoomed-in view of three of the pulse responses for the small production rate. Each pulse acts like a short well test, and the figure shows Δt and ΔP since the start of the pulse (start times of pulses are shown in **Figure 10).** The pulse response is notably larger after the CO_2 arrives at the monitoring well. There are two factors contributing to the change: (1) relative permeability effects cause the pressure response to pumping to increase, and (2) the lower density of the CO_2/brine mixture being produced requires a larger volumetric flow rate to achieve the specified constant mass production rate. The effect of the partially closed lateral boundary (an upturn in ΔP at late times) is later after the CO_2 arrives, because the two-phase system has a larger compressibility than the single-phase brine.

Note from **Figure 10** that the arrival time of the CO_2 plume at the monitoring well for the injection-only case is about 5.5 days, whereas previous studies with the Version 0 model, using the same fluid properties and injection rate, calculated an arrival time of about 3 days. Table 1 summarizes how features of the new 2D model affect CO_2 arrival time at the monitoring well.

Table 1. Comparison of features of the 2D and 3D models and their effect on CO_2 arrival time at the monitoring well

Model Difference	Effect	CO_2 Arrival Time at Monitor Well
2D grid has finer lateral resolution	Less numerical dispersion	Later arrival (and sharper front)
No upward coarsening sand (2D grid has one layer with one permeability)	No preferential flow into coarser sand, no buoyancy flow to top of sand	Later arrival
No thin shale (2D grid has closed boundary instead	No pressure leakage into sand above shale → higher P in sand → higher density CO_2 → smaller plume	Later arrival (very small effect)
No gaps in thin shale (2D grid has closed boundary instead)	No CO_2 leakage into sand above thin shale	Earlier arrival (insignificant effect)

To further compare the behavior of the 2D and 3D models, several variations of the 3D Version 0 model were used to simulate the CO_2 injection period. Results are shown in **Figure 13**. Each case considers injection only, with no production at monitoring well. The original vertical permeability k_v of the thin shale overlying the injection interval allows significant pressure release, whether or not there are gaps in the shale. Decreasing k_v in the shale by 100 increases the pressure response below the shale and decreases the pressure response above the shale, but does not affect CO_2 arrival time. On the other hand, the presence of the upward-coarsening sand in the 3D model does affect CO_2 arrival time; for a model with uniform permeability, the arrival time is about 1.5 days later, owing to the absence of preferential flow through the shallowest portion of the upward-coarsening sand.
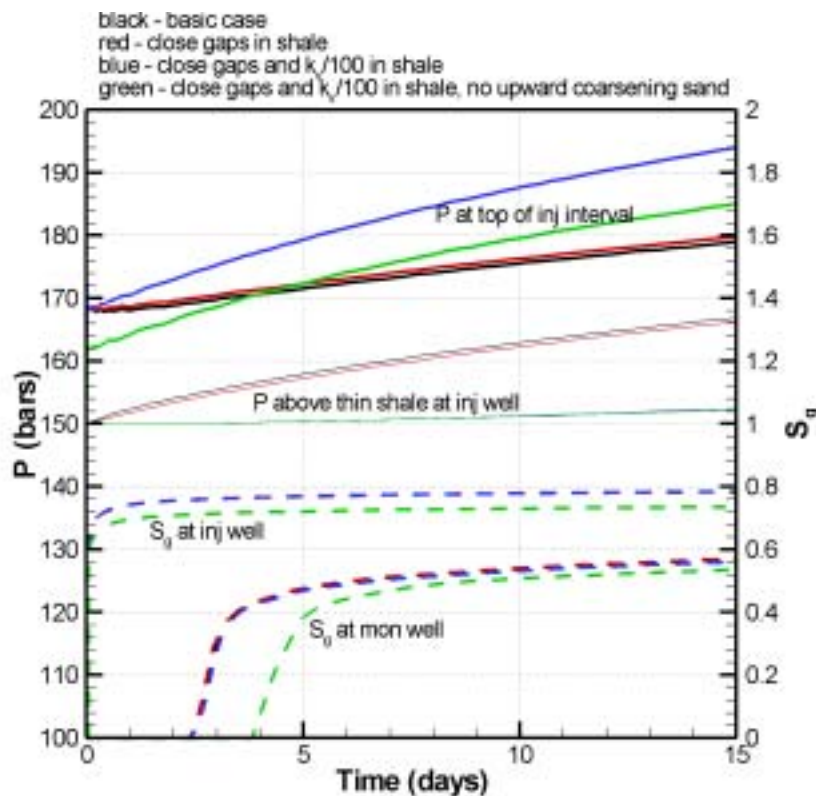

Figure 13. Results of several variations of the 3D model for CO_2 injection. The base case is the Version 0 model with Frio-like relative permeability curves, described in previous reports.

In conclusion, neither constant nor pulsed production at the monitoring well has a large effect on plume evolution, although production slightly shortens transit time of CO_2 from the injection well to the

monitoring well. Pulsed production may provide additional information on system behavior by creating pulse tests for pressure-transient analysis. Comparing results of 2D and 3D models has elucidated the various effects controlling CO_2 plume evolution, and indicated that it is necessary to use a 3D model to capture all the physical processes affecting the plume.

Further details of these studies may be found on BEG's Reservoir web site for the Frio Brine Pilot, under TOUGH2 simulations/Injection-Scenarios.ppt.

Include Heat Flow and Temperature Changes in CO_2 Injection Simulation

The TOUGH2 modeling of the Frio Brine Pilot described in previous quarterly reports has included just the formation level and has been done under isothermal conditions. This is because isothermal simulations are computationally efficient, and thermal effects at the formation level accompanying CO_2 injection are expected to be small. In contrast, thermal effects in the injection well between the ground surface and the formation level are expected to play a large role in determining the phase composition and physical properties of the injected CO_2 when it reaches the formation level. Simulated wellbore behavior is described in **Appendix B**. Here, we include heat flow and temperature changes in a simplified radial model of the formation into which CO_2 is injected, and compare the results to comparable isothermal simulations to check whether the isothermal approach is adequate.

The one-dimensional radial model consists of a 6 m thick layer with a permeability of 286 md, a porosity of 28%, Corey relative permeability curves with residual saturations $S_{lr} = 0.02$ and $S_{gr} = 0.23$ for the liquid and gas phases, respectively, and a capillary pressure function developed specifically for Frio sandstones. Initial formation conditions are P = 150 bars, T = 64°C, and salinity of 100,000 ppm ($X_{NaCl} = 0.1$). CO_2 is injected at a constant rate of 3 kg/s for 15 days.

Figures 14 to 16 show the model results for 7.5 days, the time that CO_2 arrives at the monitoring well, for an isothermal case, a non-isothermal case in which injected CO_2 has the same temperature as the formation, and a more realistic non-isothermal case in which cooler CO_2 is injected. Aside from the temperature profiles, there is very little difference between the various cases. Pressure increases in response to CO_2 injection. The supercritical CO_2 partitions into an immiscible gas phase (S_g) and partially dissolves in the aqueous phase (X_{CO2L}). There is a small counterflow of brine and water vapor near the well (not shown), with brine driven toward the well by capillary forces and water vapor driven away from the well by the pressure gradient. As brine vaporizes close to the well, it leaves behind its dissolved salt, so the salinity of the remaining brine (X_{NaCl}) increases and salt precipitates (S_s). Liquid-phase diffusion is not included in the simulation, making the X_{NaCl} profile unrealistically sharp. When thermal effects are considered, the amount of dissolved CO_2 changes slightly, in accordance with the temperature-dependence of CO_2 solubility. When cooler CO_2 is injected, brine-vapor counterflow is smaller, so less salt precipitates near the well.
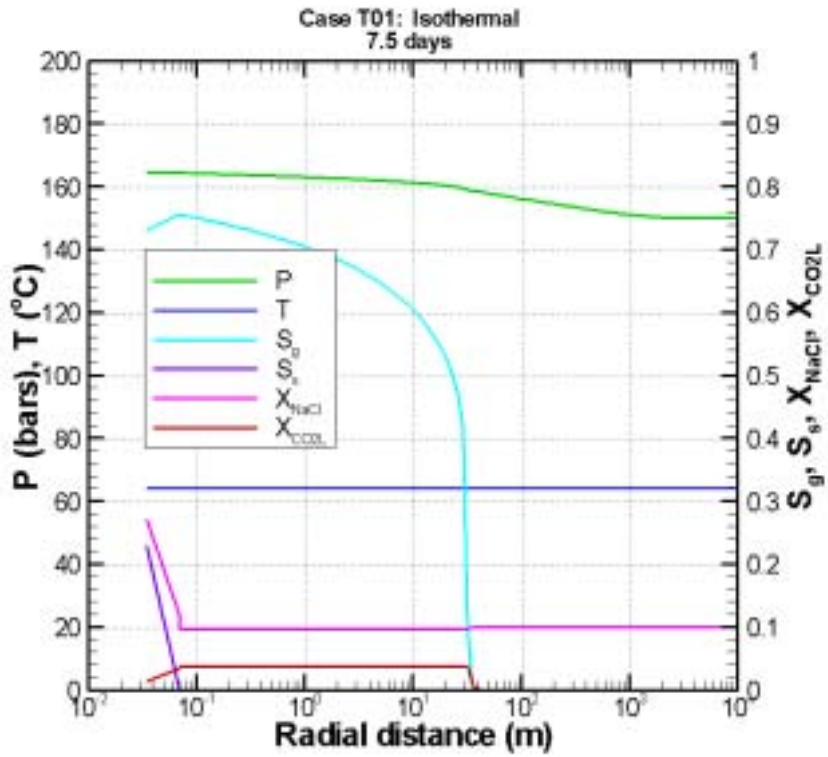
Figure 14. Isothermal radial model results after 7.5 days of CO_2 injection. Variables shown are pressure (P), temperature (T), gas saturation (S_g, almost entirely immiscible CO_2, along with a small amount of water vapor), precipitated salt saturation (S_s), mass fraction of salt dissolved in the brine (X_{NaCl}), and mass fraction of CO_2 dissolved in the brine (X_{CO2L}).
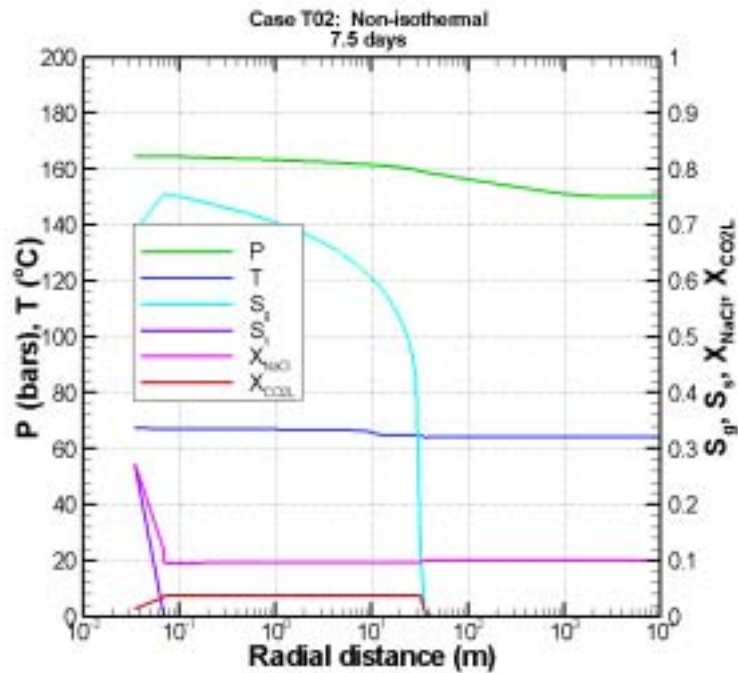

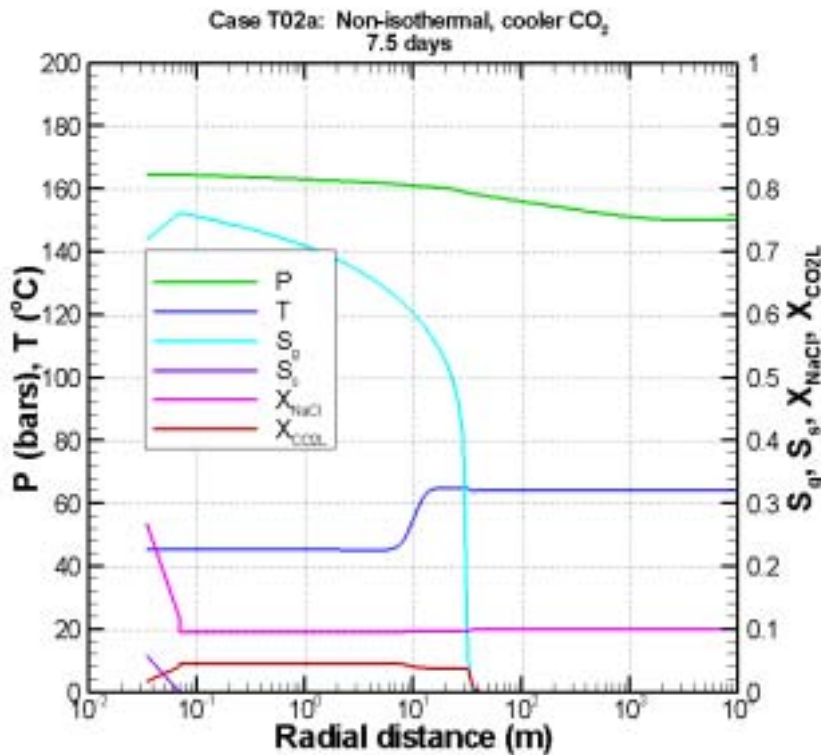**Figure 15.** Non-isothermal model results after 7.5 days of injection of 64°C CO_2.

Figure 16. Non-isothermal model results after 7.5 days of injection of 44°C CO_2.

These simulation results confirm that using an isothermal model for CO_2 behavior at the formation level is reasonable. However, it is important to consider thermal effects when describing CO_2 behavior between the ground surface and the formation level, as demonstrated by wellbore simulations (see Appendix B).

Study of CO_2 Plume Evolution Using Hysteretic Characteristic Curves

Previous numerical modeling studies (see September–November 2002 and December 2002–February 2003 Quarterly Reports) have indicated that the choice of relative permeability curves has a strong impact on CO_2 plume development and movement in the subsurface. In particular, a small value (~0.05) of residual gas saturation S_{gr} causes a diffuse plume with a relatively low value of S_g to form during CO_2 injection, and this residual gas saturation allows the plume to spread and move significant distances after CO_2 injection ceases. In contrast, a large value (~0.25 – 0.30) of S_{gr} creates a more compact plume with a higher value of S_g, which does not move much after injection ceases. This difference in behavior has significant ramifications for conceptualization and design of CO_2 sequestration scenarios. Some disagreement has arisen over which size S_{gr} more realistically represents flow and transport processes involving supercritical CO_2 and brine. Pore-scale studies suggest that the value of S_{gr} actually depends on the state and history of the flow system. The CO_2 injection period, when the CO_2 plume is growing in the subsurface, mainly represents a drying process in which the nonwetting phase (supercritical gas-like CO_2) advances into previously brine-filled pores, and a small value of S_{gr} is appropriate. After CO_2 injection ceases, the CO_2 plume moves under the influence of gravity, and at the trailing edge of the plume, rewetting occurs. It is here that the possibility of CO_2 trapping arises, which is represented by a large value of S_{gr}. Moreover, the magnitude of S_{gr} at a given location should increase with the maximum S_g experienced at that location, as large values of S_g imply that CO_2 has penetrated into smaller pore spaces as well as the more easily accessed large pores.

Figure 17 shows the nonhysteretic relative-permeability curves that have been used for previous modeling studies to investigate the impact of S_{gr}. Note that the overall shapes for the two sets of curves is similar, but that there is a shift along the horizontal saturation axis that results from the different values of S_{gr} and S_{lr} used. This shift essentially changes the saturation values at which fluids are mobile. In particular, with a large S_{gr} (Frio-like curves), during CO_2 injection S_g must reach high values before the CO_2 can move out into the formation. After injection ceases, it only takes a small decrease in S_g accompanying plume spreading for the plume to become immobile. With a small S_{gr} (generic curves), the opposite holds: during CO_2 injection, the plume can grow with a small S_g, and after injection, S_g can decrease significantly before the plume becomes immobile. Our general understanding is that the low-S_{gr} generic curves are more appropriate during plume injection, and the high-S_{gr} Frio-like curves are more appropriate during post-injection plume evolution. However, this assessment is an oversimplification: during CO_2 injection periods, buoyancy flow can cause plume movement that results in rewetting, and during post-injection periods, the leading edge of the CO_2 plume can continue the drying process, indicating that simply using different relative permeability curves for different time segments of a simulation would not be adequate. A unified approach that better represents pore-scale wetting and drying processes is needed. Capillary pressure and relative permeability curves that are both state- and history-dependent (i.e., hysteretic) provide a means to address this need.
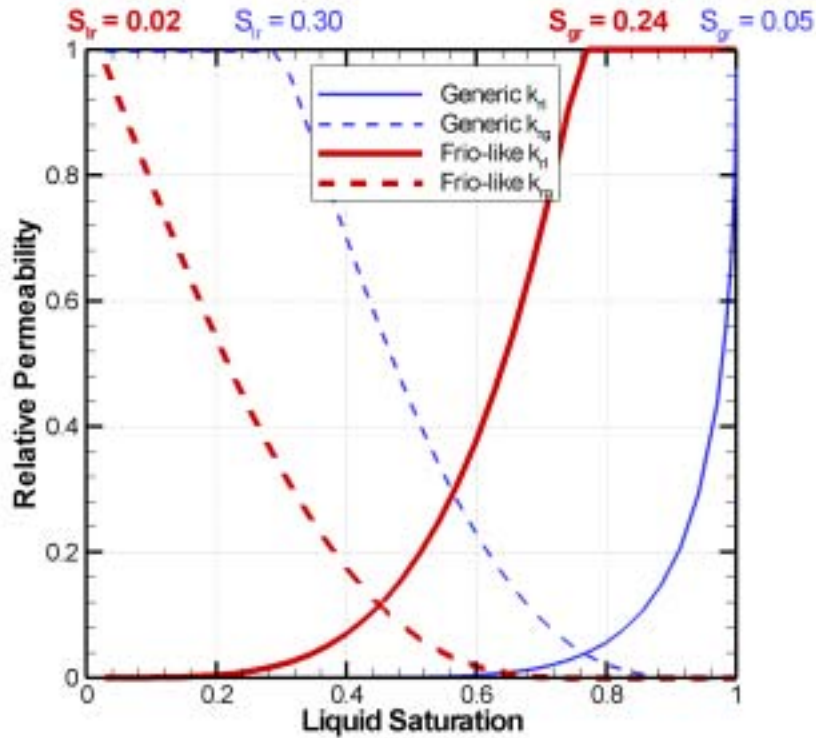

Figure 17. Nonhysteretic relative permeabilities used for previous modeling studies of CO_2 plume formation and movement

A version of TOUGH2 that incorporates hysteretic capillary pressure and relative permeability curves, along with nonwetting phase trapping, is being adapted and applied to CO_2 sequestration simulations. Results are preliminary so far, and there are indications that numerical difficulties need to be overcome, but the formulation accounts for all the physical processes believed to be significant. For example, **Figure 18** shows S_{gr}^{Δ}, the history-dependent value of S_{gr}, as a function of S_{gi}, the initial value of S_g for the current rewetting process. Consider the rewetting that occurs after CO_2 injection ceases. For most gridblocks, S_{gi} is the local value of S_g when injection ceases. Near the edge of the CO_2 plume, S_{gi} is small, so according to **Figure 18**, S_{gr}^{Δ} is small, too. In contrast, near the injection well, S_{gi} and consequently S_{gr}^{Δ} are large.
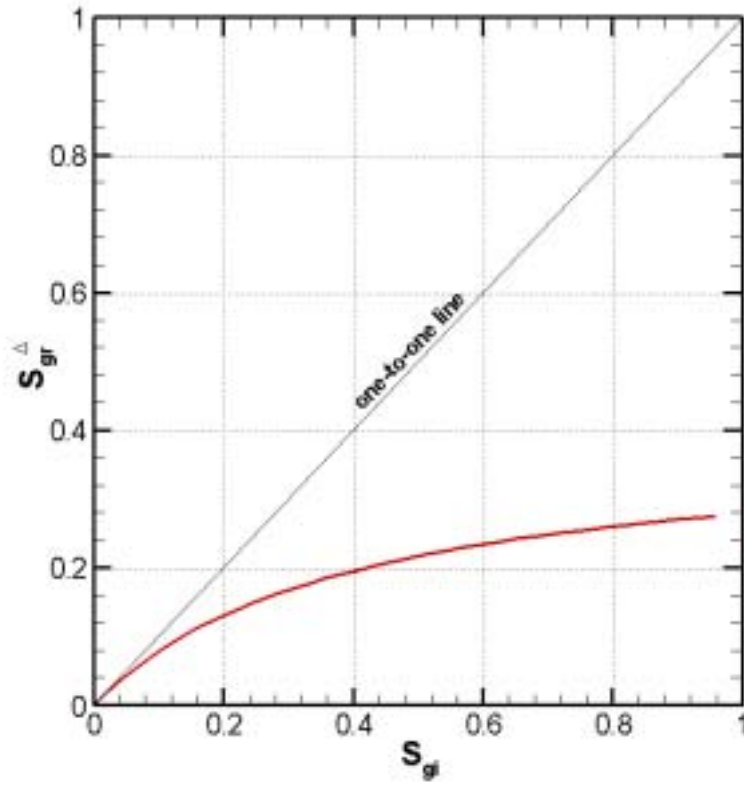
Figure 18. S_{gr}^{Δ}, the history-dependent value of S_{gr}, as a function of S_{gi}, the initial value of S_g for the current re-wetting process.

Figure 19 shows the hysteretic capillary pressure and relative permeability functions obtained at the model locations corresponding to the injection and monitoring wells for a simplified 2D (one-layer) model of the Frio Brine Pilot. Fifteen days of CO_2 injection are followed by 35 days of rest. The initial state of the system contains no CO_2, so $S_l = 1$, $P_{cap} = 0$, $k_{rl} = 1$, and $k_{rg} = 0$. During CO_2 injection, drying of the formation occurs, first at the injection well and later at the monitoring well, with both locations following the same characteristic curves (since both start with the same initial conditions). After 15 days, injection ceases and rewetting begins at both wells. Because S_{gi} for rewetting is much larger at the injection well than at the monitoring well (compare S_l values for the red and green "turning points" in **Figure 19**), the S_{gr}^{Δ} value (**Figure 18**) is much larger also, and consequently the rewetting portions of the characteristic curves for the two locations are quite different from one another, as well as being distinct from the drying portions of the curves.

It appears from these preliminary results that the desired features of state- and history-dependent characteristic curves can be implemented in simplified models of CO_2 injection. It still remains to improve simulation efficiency enough to make employing this approach practical for the larger 3D models that incorporate more geological and operational realism.
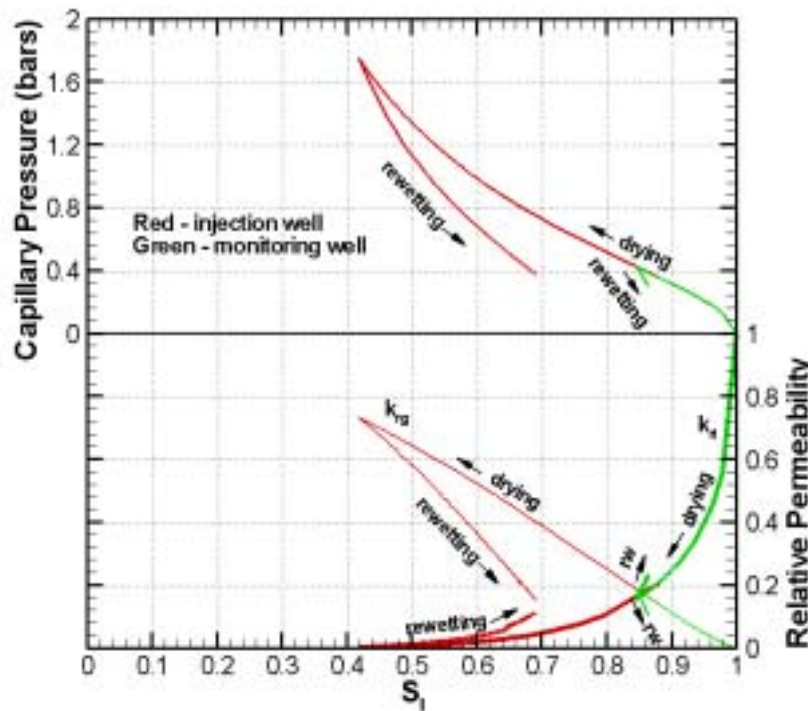
Figure 19. Hysteretic capillary pressure and relative permeability functions obtained from a simplified one-layer model of the Frio Brine Pilot test comprising 15 days of CO_2 injection and 35 days of subsequent rest

Develop and Apply Version 0.5 Model for Simulation of CO$_2$ Injection and Subsequent Rest Period

A new 3D model of the Frio Brine Pilot has been developed, the "Version 0.5" model, which incorporates more geological realism than the previous Version 0 model. The model is a tilted plane of uniform thickness, which is closed to the NE, NW, and SE, and extends far to the SW (as in the Version 0 model). A new feature is that the "C" sand thickness and porosity-depth profile, as well as the depth of the thin shale near the middle of the "C" sand, are now taken from logs of well SGH-4, the monitoring well for the pilot test. The model dips 17.5° to the south (along the line between the injection and monitoring wells). This is a new dip direction (no longer parallel to the model boundaries), one that better represents the actual warped layers that curve in two directions. Finally, a small fault near the monitoring well is now included. In our base-case simulation, this fault is closed (i.e., it acts as a barrier to flow). **Figure 20** shows a schematic plan view of the fault block, and **Figure 21** shows a plan view of the grid. **Figure 22** shows the porosity-depth profile inferred from well SGH-4 logs and the discretized porosity assignment for 16 model layers. Model permeabilities k_h and k_v and characteristic curve parameters are taken from correlations with porosity ϕ, developed from core analysis on Frio (not specific to South Liberty) samples and literature information. The resulting relative permeability functions have high values of S_{gr}, comparable to the Frio-like curves shown in **Figure 17**. Average model properties are given in **Table 2**.

Table 2. Average model properties for the Version 0.5 model of the "C" sand

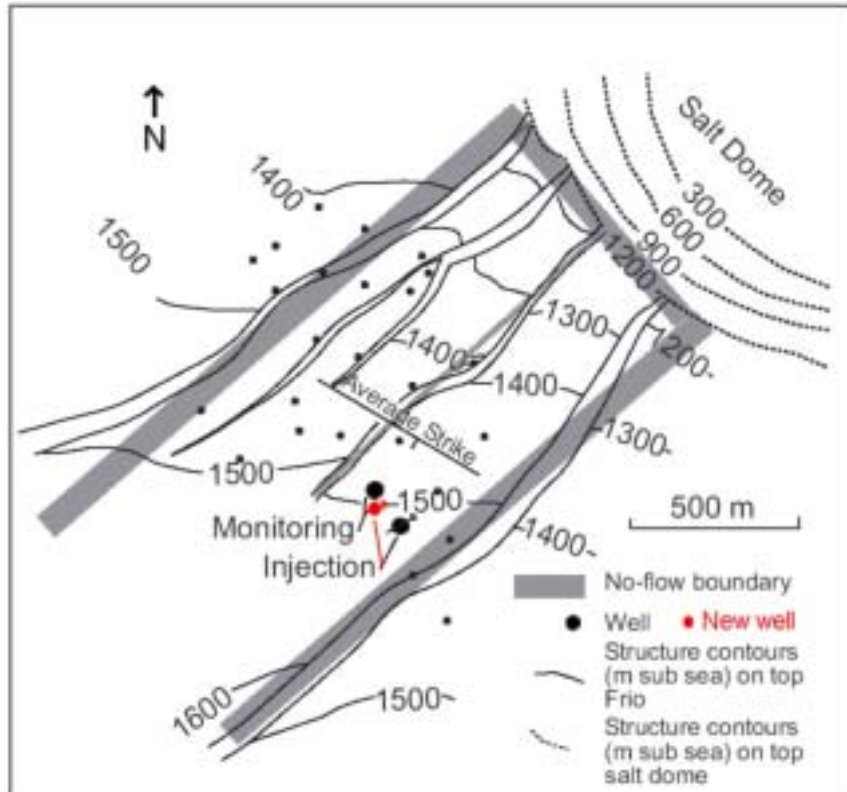| Zone	Δz	ϕ	k_h (md)	Range of k_h (md)
Upper sand	11 m (36 ft)	0.24	49.4	0.004 – 156
Thin shale	2 m (6 ft)	0.05	0.01	0.01
Lower sand	14 m (47 ft)	0.28	50.4	3.4 – 105

Figure 20. Schematic view of the South Liberty fault block and the closed (no-flow) boundaries of the Version 0.5 model
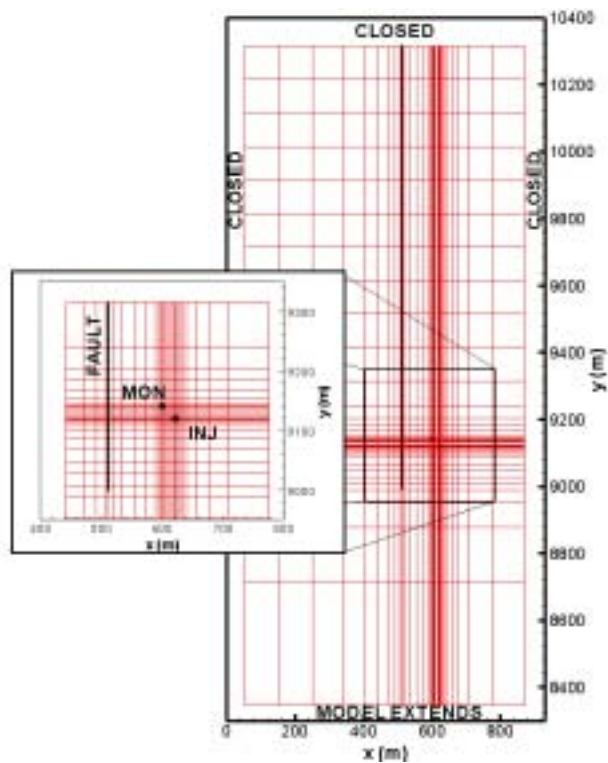

Figure 21. Plan view of the grid for the Version 0.5 model
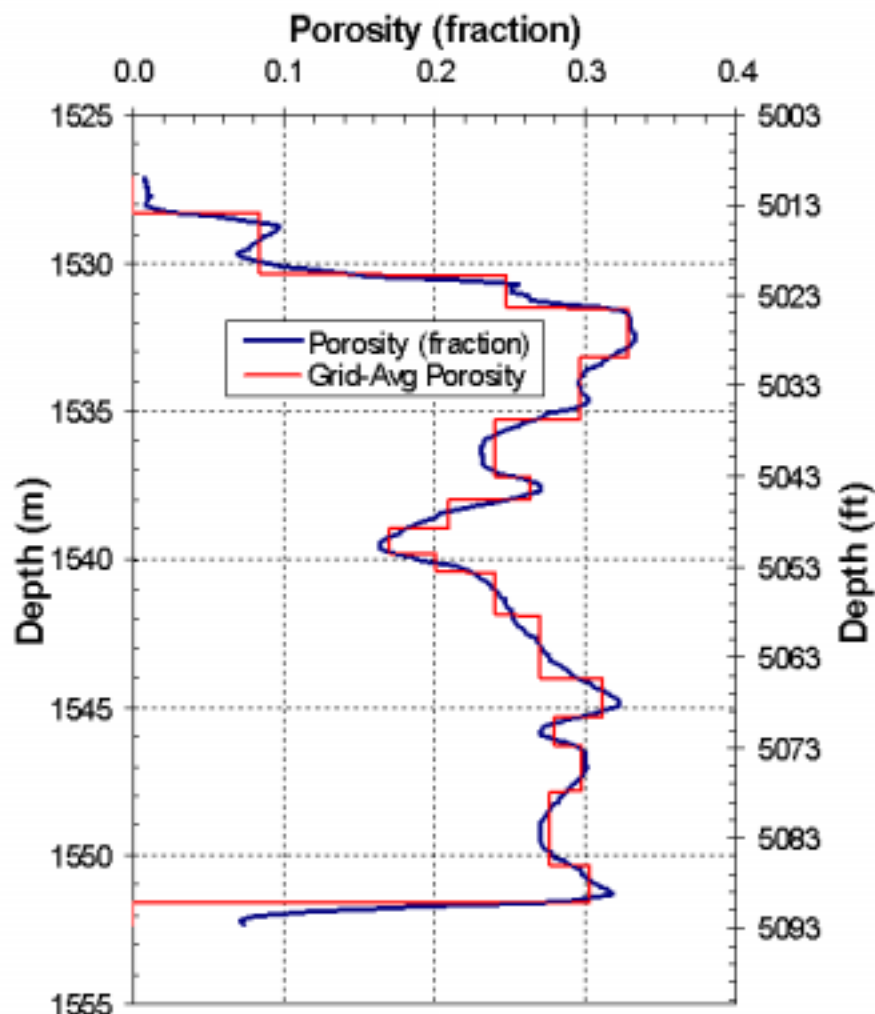
Figure 22. Porosity-depth profile inferred from well logs for well SGH-4, along with the grid-averaged values used for the Version 0.5 model

As in previous simulations, we simulated injection of 250 T/day of CO_2 for 15 days (3,750 T total), and then let the system rest. Our base-case simulation considers injection in the upper sand, above the thin shale layer. **Figure 23** shows modeled pressure, gas saturation, and dissolved CO_2 evolution during the CO_2 injection period at the injection and monitoring wells for the base case. The CO_2 plume arrival at the monitoring well is at about 6 days, significantly later than predicted by the Version 0 model (3 days), due to the greater thickness of the layer into which injection occurs (11 m versus 6 m) and lower maximum permeability. The arrival of the dissolved CO_2 (X_{CO2L}) precedes the arrival of the immiscible CO_2 (S_g) by several days, suggesting interesting possibilities for monitoring. **Figure 24** shows the long-term evolution of these quantities after injection ceases. Additional simulations consider injection in the lower sand, treat the small fault as a constant-pressure boundary, use alternative relative permeability curves, or assume that the thin shale layer is missing. **Table 3** summarizes CO_2 arrival times and maximum pressure changes for all the alternative models. Note that CO_2 arrival is earlier for the generic relative permeability (**Figure 17**), due to the lower gas saturation within the plume that causes the plume to grow faster. CO_2 arrival is much later for injection in the lower sand, a consequence of the greater thickness of high-permeability sand (**Figure 22**). This late arrival time is the primary reason we have chosen the upper sand as our preferred target for CO_2 injection. Modeling the small fault just beyond the monitoring well as an open rather than closed boundary shortens the time to CO_2 arrival at the monitoring well somewhat, because the constant pressure of the fault draws the CO_2 plume toward it. The maximum pressure change in the model is also notably lower for this case, because the open fault provides pressure relief. The absence of the thin shale layer does not impact CO_2 arrival significantly, because injection is still

limited to the depth interval of the upper sand, and buoyancy flow counters the tendency for the injected CO_2 to spread deeper.

Table 3. Summary of CO_2 arrival time at monitoring well (t_{bt}) and maximum pressure change in the model (ΔP_{max}) for the basic Version 0.5 model and several alternatives. Unless otherwise noted, each case includes Frio-like relative permeability curves, injection into the upper sand, a closed small fault, and the thin shale layer.

Case	t_{bt} (days)	ΔP_{max} (bars)
Base case	6.0	36
Generic relative permeability (small S_{gr})	3.0	32
Inject in lower sand	11.2	32
Open small fault	5.5	32
Open small fault, generic relative permeability	2.9	29
No thin shale layer	6.4	27
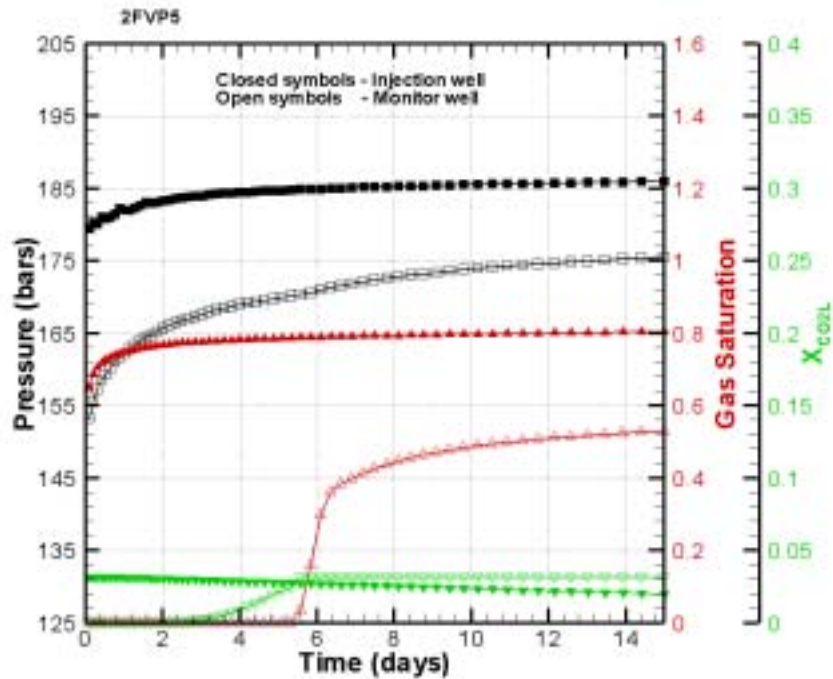
Figure 23. Modeled pressure, gas saturation, and CO_2 mass fraction in the liquid phase during CO_2 injection for the base case of the Version 0.5 model
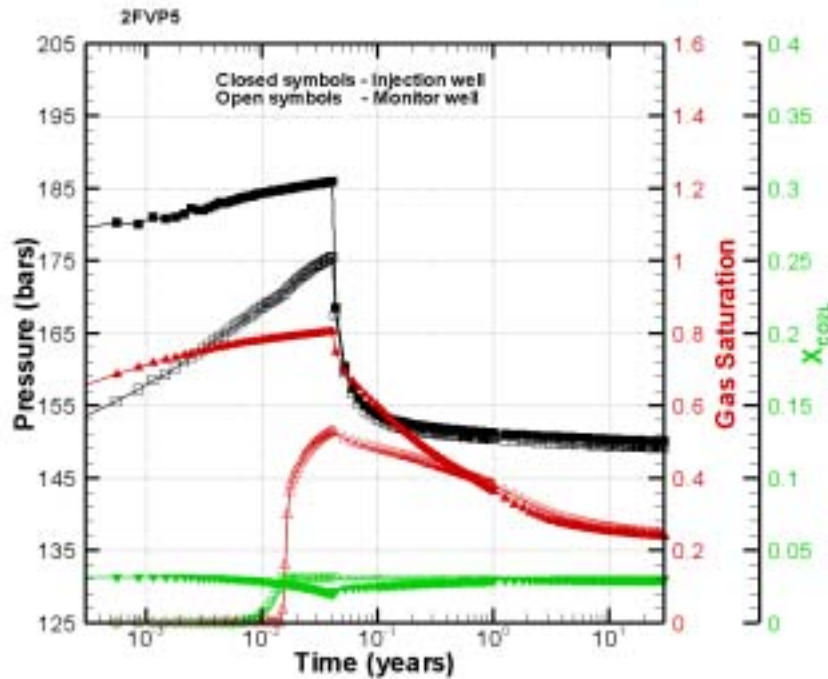
Figure 24. Modeled long-term responses to the 15-day CO_2 injection period for the base case of the Version 0.5 model.

Figure 25 shows a plan view of the pressure distributions in the highest-permeability layer of the upper "C" sand, where the extent of the injected CO_2 is the greatest. The pressure distribution for 15 days, the end of the injection period, shows that during injection, the CO_2 plume is driven radially outward from the injection well. After one year, the pressure distribution has essentially returned to its undisturbed, pre-injection state, with the combination of the formation dip and the small fault-control plume movement. **Figure 26** shows the same plan view of the immiscible CO_2 plume at four times during the injection period. The radially symmetric plume development predicted by the pressure distribution is apparent, although the rectangular grid (**Figure 21**) provides some artificial preferential flow parallel to the grid axis directions. **Figure 27** shows the CO_2 plume in a vertical cross section along the N-S line joining the injection and monitoring wells. The preferential flow through the layer with the highest permeability (z = 1,532 m; see Figure 13) is apparent. **Figures 28 and 29** show plan view and cross section, respectively, for the long-time evolution of the plume. Note that the color scale is different for the long-time figures. Because of the high residual gas saturation (S_g = 0.22 to 0.31 for the upper "C" sand layers), plume movement after CO_2 injection ceases is extremely slow.

Further details of these studies, including saturation distributions for some of the alternative simulations listed in **Table 3**, may be found on BEG's Reservoir web site for the Frio Brine Pilot, under TOUGH2 simulations/version0p5.ppt.
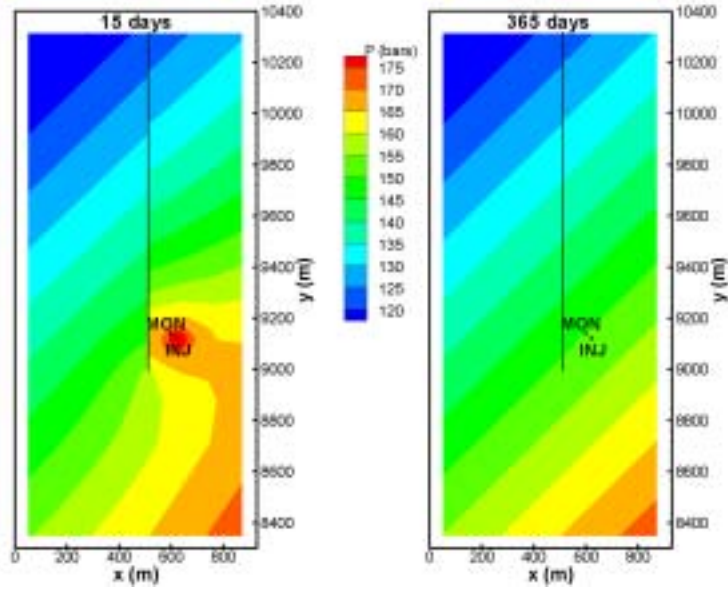
Figure 25. Version 0.5 model results: Plan view of the pressure distribution at the end of the 15-day CO_2 injection period and after one year, for the depth of maximum CO_2 plume extent
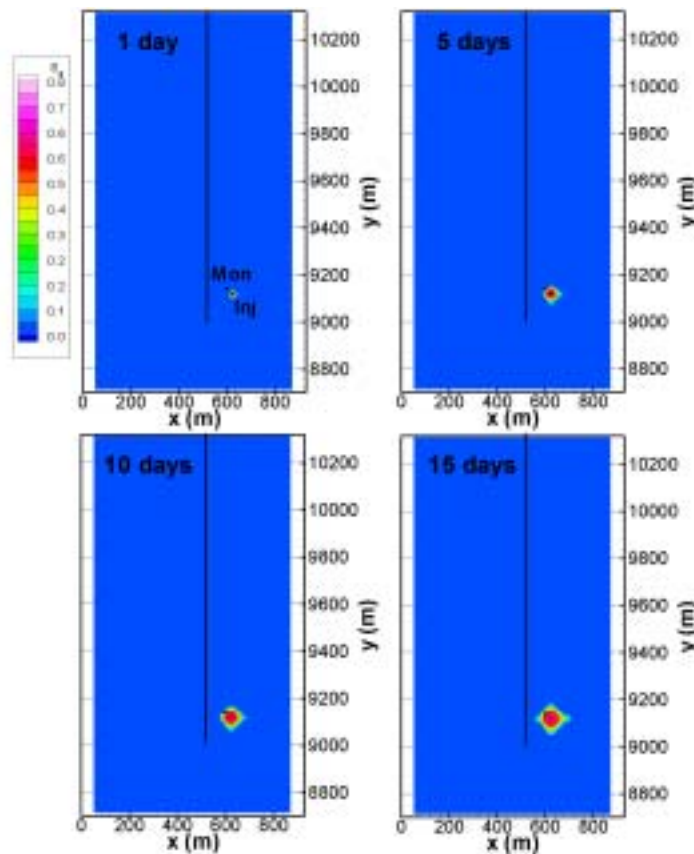

Figure 26. Version 0.5 model results: Plan view of the base-case gas saturation distribution at four times during the CO_2 injection period, for the depth of maximum CO_2 plume extent
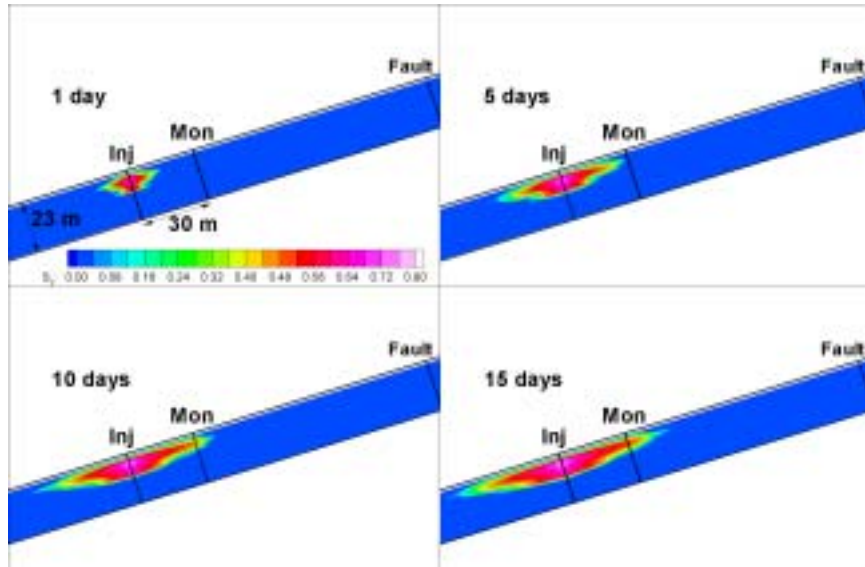
Figure 27. Version 0.5 model results: Base-case gas saturation distributions in a cross section along the N-S line between the injection and monitoring wells at four times during the CO_2 injection period
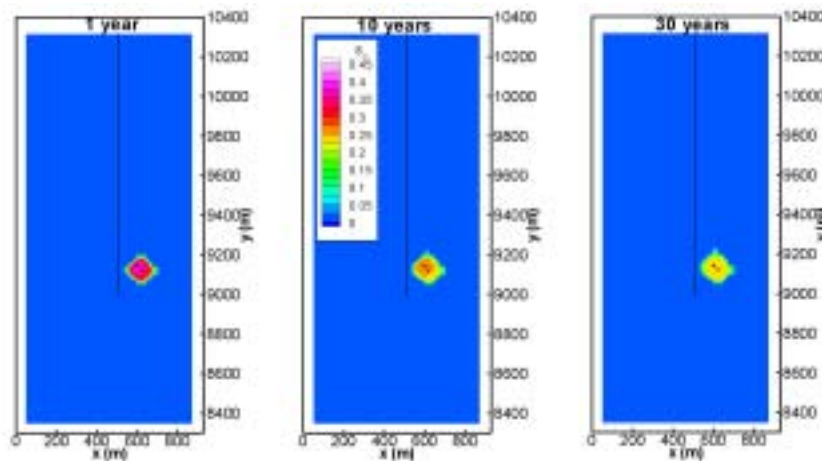

Figure 28. Version 0.5 model results: Plan view of the base-case gas saturation distribution at long times, for the depth of maximum CO_2 plume extent
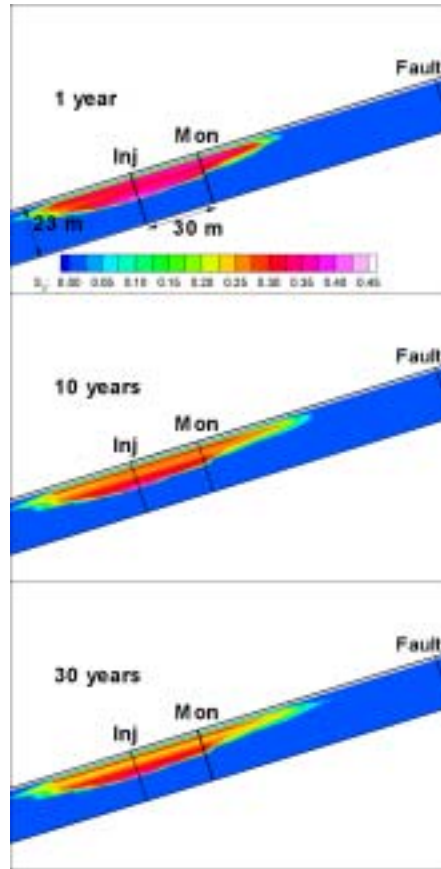
Figure 29. Version 0.5 model results: Base-case saturation distributions in a cross section along the N-S line between the injection and monitoring wells at long times.

Work Next Quarter

Further numerical simulations of the planned Frio Brine Pilot are to be conducted at the South Liberty field, incorporating more detailed test specifications as they are developed. We will focus on two areas in particular: (1) simulating a new design proposed for site characterization well testing and (2) improving the hysteretic version of TOUGH2.

Task E: Frio Brine Pilot Project

Goals

To perform numerical simulations and conduct field experiments at the Frio Brine Pilot site, near Houston, Texas, that:

➢ Demonstrate that CO_2 can be injected into a saline formation without adverse health, safety, or environmental effects.
➢ Determine the subsurface location and distribution of the cloud of injected CO_2.
➢ Demonstrate understanding of conceptual models.
➢ Develop the experience necessary for the success of large-scale CO_2 injection experiments.

Note: This task does not include work being done by BEG under the project "Optimal Geological Environments for Carbon Dioxide Disposal in Brine Formations (Saline Aquifers) in the United States," funded under a separate contract.

Previous Main Achievements

➢ An initial planning workshop was held at BEG (Austin, Texas) on July 8–9, 2002, to explore the interrelationships among the modeling and monitoring techniques proposed by the GEO-SEQ team for conducting the Frio Brine Pilot experiment. A time line and a more detailed plan for implementation of modeling and monitoring techniques were developed.
➢ Permit preparation for the project has been completed, with substantive input from the GEO-SEQ team.

Accomplishments This Period

➢ GEO-SEQ team members have contributed to preparation of the Class V well application to the Texas Commission on Environmental Quality.

Progress This Period

The BEG team and Field Service Provider Sandia Technologies worked closely with the GEO-SEQ team to develop information requested by the Texas Commission on Environmental Quality (TCEQ) Underground Injection Control (UIC) Division, in order to obtain approval to drill the injection well for the Frio Brine Pilot site.

The permitting strategy for the injection well was initially unclear. The well is sited within an oil field, and such wells are normally permitted under Texas Railroad Commission rules. However, the injection well is not intended to enhance oil production or dispose of pre-refinery oil field waste, and is therefore not eligible for a Class II permit.

The site is within an oil field featuring numerous well penetrations and nearby faults. Although this setting was deliberately selected to optimize this experiment, it is not the type of environment that would normally be selected for siting a Class I nonhazardous disposal well. The Class I construction and plug and abandon protocols are also costly, relative to the brief duration of the injection period, and may not be a careful use of public monies that are expended to support this project. In addition, the benign character of the injectate (food-grade CO_2), the experimental nature of the project, the close monitoring using multiple measurements, and the careful experimental design to minimize risk to health, safety, and the environment—all led to the proposal for a Class 5 experimental injection application. In addition to the Class 5 application, TCEQ requested that the team provide a detailed report to demonstrate adequate well design and make information available to the public. This report includes relevant information and well engineering data, following the outline of a Class I permit.

Information developed for the pilot test had to be reformatted and reorganized to fit the formats used by regulators and fill in missing elements. This included TOUGH2 simulations prepared by Christine Doughty (Berkeley Lab) and estimates of injectate compatibility based on the work of Kevin Knauss (LLNL).

In addition, BEG developed and made information available to the public. Susan Hovorka presented an overview of the project to Dayton community leaders and to the local press on June 19, 2003, at the Dayton Rotary Club, and did a walking canvass of the neighborhood along CR 460 (Dugat Road) to provide information to residents. Materials were prepared and made available on a Website (see http://www.beg.utexas.edu/environqlty/co2seq/fieldexperiment.htm).

In early August, Sandia Technologies and subcontractors, in collaboration with BEG researcher Shinichi Sakurai, entered and assessed the casing of the proposed monitoring well SGH#4. The condition of the casing was found to be good, and a cement bond log was run by Schlumberger to help develop the plans for a cement squeeze to isolate the injection zone.

Work Next Quarter

Next quarter, we will finalize and submit the report to support the Class 5 permit application to the Texas Commission on Environmental Quality.

Appendix A

ORNL's Input on Sampling and Analysis for the Frio Injection Test

Background

This information was provided to Alan Dutton of BEG by LBNL (Mack Kennedy), LLNL (Kevin Knauss and Jim Johnson), and ORNL (Dave Cole and Tommy Phelps).

Sample Integrity and Preservation are of Principal Importance

The sample and analysis plan outlined below is predicated on a number of assumptions regarding the drilling and injection plan put forth during the April meeting in Houston sponsored by BEG, with additional modifications currently pending final discussion.

a. The April 9th spreadsheet of Mike Hoversten summarizing the drilling and injection plan is still an accurate guide for the test.
b. Core samples will be available from the drilling of the injection well.
c. Based on the April plan, we can anticipate three injection episodes—a one-day injection, a three-day injection, and an 11-day injection, with a two-day hiatus between the first two and a five-day hiatus between the second and third injections.
d. Routine on-site chemical analyses and sample (gases and fluids) preservation will be provided by staff from TBES and/or the USGS (Yousif Kharaka).
e. In addition to gases and fluids sampled during continuous flow of the well during and after injection, some downhole samples will be obtained via the USGS sampler that can help us test the usefulness of the well-head gas, fluid and isotope chemistries.
f. Access will be provided to the wellhead, so that noble and perfluorocarbon tracer gases (PFTs) can be introduced into the CO_2 stream during the injection episodes.
g. Continued access will be provided to the system during the post-injection monitoring, so that samples can be obtained over periods of several months to perhaps as long as a year. Long-term sampling will be supported by staff at BEG and may be the USGS.

Samples and Chemistries of Interest

➢ Gas species—free gas as well as dissolved gas species; CO_2, CH_4, higher hydrocarbons; H_2S, noble gases (e.g., He, Ar, Kr, Xe), and their isotopes, introduced PFTs
➢ Fluids—major and minor cations, major and minor anions, pH, alkalinity, TDS, DOC, dissolved organic species, stable isotopes (O, H, C, S), $^{87}Sr/^{86}Sr$
➢ Core—mineralogy, major, minor and trace element chemistry, stable isotope chemistry of detrital and diagenetic phases, $^{87}Sr/^{86}Sr$, porosity and permeability

On-Site Laboratory Assignments

➢ BEG/USGS—wellhead sample collection and preservation of fluids and gases; routine chemical characterization (e.g., pH, alkalinity, TDS)
➢ USGS—as above, plus downhole sampling and preservation (Kharaka)
➢ LBNL—noble gas introduction during CO_2 injection (Kennedy and Pruess)
➢ ORNL—PFT introduction and analysis (if possible) during and after CO_2 injection (Phelps)
➢ LLNL—On-site fluid chemistry and sample preservation, if not covered by USGS or BEG (Knauss)

Off-Site Laboratory Assignments

➢ LBNL—noble gas chemistry and isotope analysis (POC—Mack Kennedy)
➢ ORNL—gas chemistry and stable isotopes; water isotopes; dissolved species isotopes, isotopic characterization of core (Cole); PFT gas analysis (Phelps). (Characterization of the solids collected during drilling that the staff members at the BEG plan not to address in their studies of the core.)

- ➢ BEG—major, minor and trace element chemistry of fluids and solids, mineralogy & physical characterization of core
- ➢ LLNL—Fluid chemistry if BEG needs help (Knauss)

Sample Handling and Amounts

- ➢ Carbon-based gases—500 cc or 1 L stainless steel high pressure cylinders with standard ¼" NPT fittings and valves
- ➢ Noble gases— ~10 cc of free gas and/or water, which will be collected either in flow through Cu tubes with cold weld seals or pre-evacuated 10 cc cylinders with fittings designed to match the sampling equipment
- ➢ Gases for PFTs— 10–15 cc; analysis to be performed off-site with GC
- ➢ Fluids—1 L glass bottles; minimum of several liters for various chemical and isotopic analyses; on-site chemical acidification for some analyses; chemical treatment for capture and preservation of dissolved species for isotope analyses (e.g., Zn acetate to separate reduced sulfur)

Sample Frequency: (Ultimately predicated on the injection scenario and funding!)
(Sample defined as equal to one gas and one fluid/well-head sampling event)
(The frequency of downhole sampling is predicated on time needed for the tool to descend and return to the surface)

- ➢ Pre-injection sampling—minimum of two samples from each well on the two days preceding the first CO_2 injection to establish a baseline
- ➢ Injection sampling—plan calls for flowing the well ~23 times in the first 11days (includes injection episodes 1 and 2), so at minimum we need this many samples. Probably need a minimum of 2 – 3 samples per day during the third major injection (11 days); for PFTs could involve 100's of samples
- ➢ Post-Injection sampling—samples obtained on day 23 and beyond; 2-3/day for the first
Few days, then tapering off to once a day for another week?
Long-term sampling (over several months to several years)

*Note: This adds up to about 50 to 75 samples (not including the samples for PFTs). Also, this preliminary plan has not considered what to do about leakage samples for the "B" sand.

Appendix B

Wellbore Effects in CO_2 Injection
Karsten Pruess, Lawrence Berkeley National Laboratory
September 2003

Flow conditions in a CO_2 injection well (injection rate or pressure, injection enthalpy or temperature) may be controlled at the wellhead, but not directly at bottomhole ("sandface"). From an operational point of view, it is of interest to know how wellhead pressures change with time when CO_2 is injected at a prescribed rate. An analysis of pressure transients in the reservoir requires knowing the time dependence of the flow rate at the sandface, not at the wellhead. The required information can be obtained through downhole spinner measurements, at considerable expense. Alternatively, wellbore simulation may be used to deduce downhole conditions from wellhead parameters. Here, we report on a preliminary analysis of flowing conditions in a CO_2 injection well by means of numerical simulation. Problem parameters were patterned after the expected conditions at the upcoming Frio test.

As will be seen below, CO_2 flow down a wellbore is strongly impacted by non-isothermal effects. These mainly arise from an interplay between fluid flow and conductive heat exchange with the formation, but phase change between liquid and gaseous CO_2 (boiling, condensation) and heat of dissolution in the aqueous phase also play a role. We currently do not have a wellbore flow simulator available that can model multiphase flows of CO_2-water mixtures at high CO_2 partial pressures and relatively low temperatures, from ambient to 65°C or so. However, making a number of simplifying assumptions, we have been able to obtain an approximate solution to the problem using the TOUGH2 reservoir simulator. The main simplification is that frictional pressure drop in the wellbore is neglected, which should be a good approximation (Carroll and Lui, 1997). The wellbore is treated as a region with very large permeability, so that for the applied flow rate, pressure gradients in the wellbore are always very close to hydrostatic, within a fraction of one percent.

In the simulations presented below, the wellbore is modeled as a pipe of 10 cm radius (approximately 8 inches in diameter), extending from the land surface to a depth of 1,500 m. The well is held in a typical geothermal gradient of 30°C/km, with a land surface (wellhead) temperature of 20°C, so that temperature at 1,500 m depth is 65°C. The well is assumed to be water-filled initially, in hydrostatic equilibrium against an ambient wellhead pressure of 1.013 bar. Bottomhole pressure under hydrostatic conditions is then 147.206 bar.

CO_2 is injected into an initially water-filled wellbore at a constant wellhead rate of 3 kg/s, corresponding to 259.2 tonnes/day, with a constant wellhead temperature of 20°C. At the same time that CO_2 injection is started at the wellhead, bottomhole pressure is increased by 7.505 bar to 154.711 bar. This pressure adjustment was made primarily to facilitate comparison with other analyses of "static" CO_2 columns that had been done previously. Two cases were investigated, Case 1 having constant bottomhole pressure of 154.711 bar, while in Case 2 the outflow from the wellbore is fed into a 1D radial grid system that represents the target injection formation, with parameters chosen representative of the Frio formation (**Table B-1**). In Case 2, therefore, there will be some buildup of bottomhole pressure in response to fluid flow into the formation.

Table B-1. Hydrogeologic parameters

Permeability	$k = 1.5 \times 10^{-13}$ m^2
Porosity	$\phi = 0.25$
Pore compressibility	$c = 0$ Pa^{-1}
Aquifer thickness	$H = 10$ m
Relative Permeability	
Stone's first three-phase method (Stone, 1970)	
irreducible water saturation	$S_{lr} = 0.30$
irreducible non-aqueous liquid saturation	$S_{nr} = 0.05$
irreducible gas saturation	$S_{gr} = 0.05$
exponent	$n = 3$
Capillary pressure	$P_{cap} = 0$
Fluid Properties	
pressureFluid properties	$P = 154.71$ bar
temperature pressure	$T = 65^oCP = 154.71$ bar
salinity (mass fraction of dissolved NaCl) temperature	$X = 0.10T = 65^oC$
salinity (mass fraction of dissolved NaCl)	$X = 0.10$

The bottomhole pressure adjustment made at startup of CO_2 injection has very minor effects, causing spurious (unphysical) upward water flow for just a few seconds. Subsequent evolution is as follows.

In response to CO_2 injection, a free gaseous CO_2 phase evolves at the wellhead, accompanied by pressurization that propagates rapidly down the wellbore. Outflow of water at bottomhole (sandface) commences within less than a minute and initially occurs at rather high rates of around 20 kg/s, This results from the injected CO_2 being at rather low pressure initially, and therefore having low density and a corresponding large volumetric rate.

Wellhead pressures increase rapidly (**Figure B-1**), and reach 57.32 bar, the saturation pressure of CO_2 at $T = 20^oC$, after about 20 minutes for Case 1, and even more rapidly in Case 2. When saturation pressure is reached at the wellhead, CO_2 becomes a two-phase mixture of liquid and gaseous CO_2. In two-phase conditions, pressure is a unique function of temperature, and wellhead pressure remains constant at 57.32 bar as long as CO_2 remains in two-phase conditions there. Sandface flow rates go through considerable transient changes. Within less than 1 hour, the water flow rate at the sandface stabilizes to a value near 3 kg/s (**Figures B-2 and B-3**). Some fluctuations in water rates are seen, caused by space discretization effects, and are much stronger for Case 1 than for Case 2, reflecting greater sensitivity when CO_2 is present as a two-phase mixture in the wellbore.
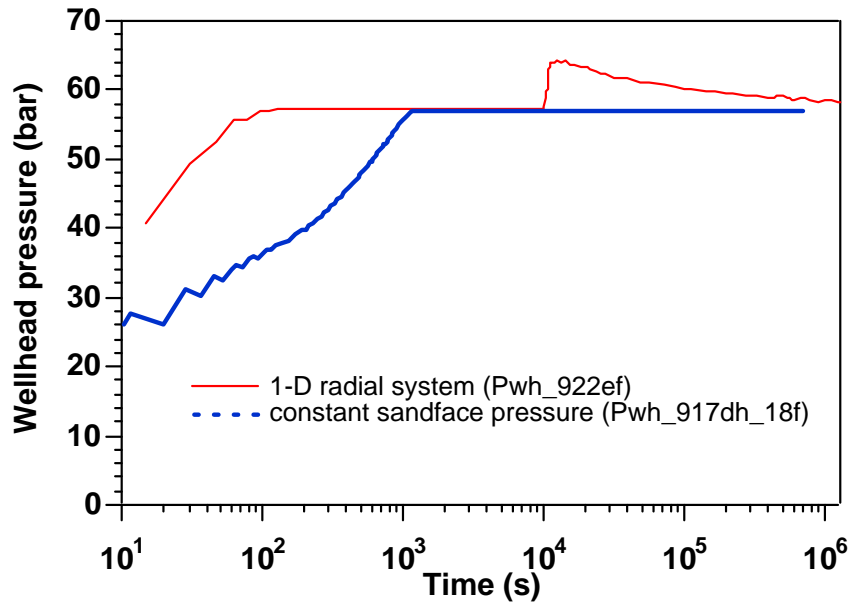
Figure B-1. Simulated wellhead pressures for CO_2 injection at constant wellhead rate of 3 kg/s
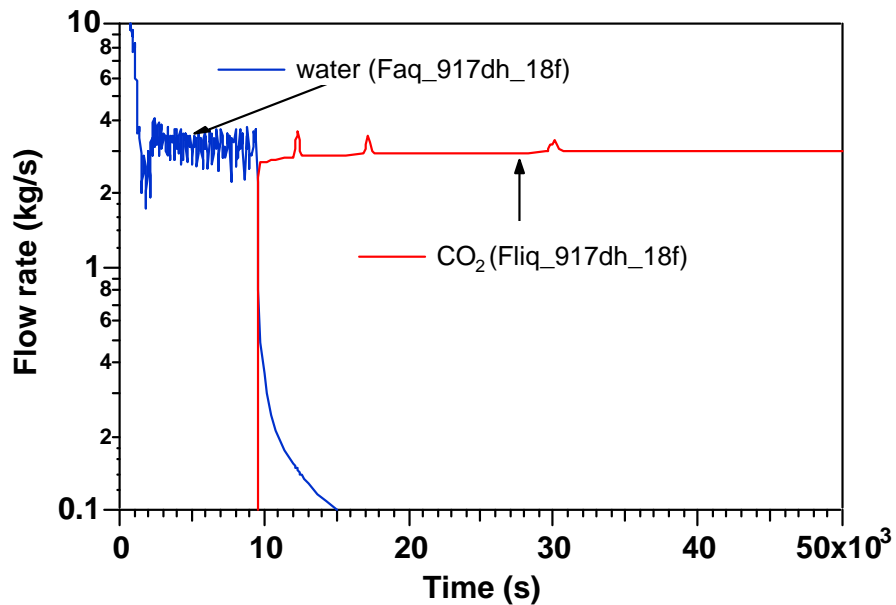

Figure B-2. Simulated sandface flow rates of CO_2 and water for CO_2 injection at a constant wellhead rate of 3 kg/s: Case 1
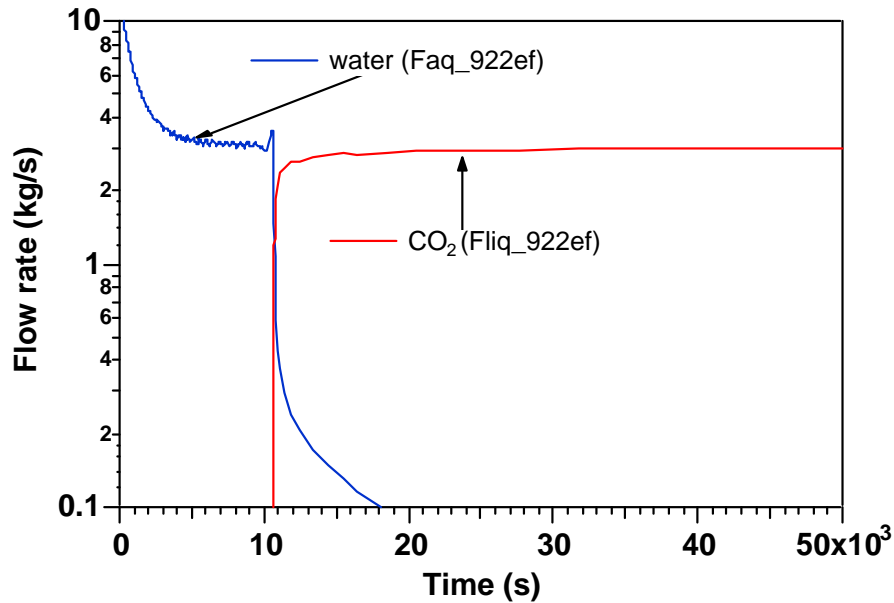
40

Figure B-3. Simulated sandface flow rates of CO_2 and water for CO_2 injection at a constant wellhead rate of 3 kg/s: Case 2

Carbon dioxide reaches the sandface in slightly less than 3 hours, consistent with a simple estimate of the time needed to inject a wellbore volume's worth of CO_2. After CO_2 breaks through at the sandface, CO_2 sandface rates quickly stabilize at a value of 3 kg/s. In Case 1, two-phase conditions are maintained at the top of the well indefinitely. In Case 2, there is complete condensation of gaseous CO_2 in the wellbore after about 3 hours, resulting from an additional pressure increase caused by reduced total fluid mobility (relative permeability effects) as CO_2 begins to exit the wellbore and enter the reservoir formation. With continuing flow of CO_2, temperatures in the wellbore continue to decline slowly (**Figure B-4**). The changing temperature and pressure conditions have a strong impact on fluid density (**Figure B-5**).
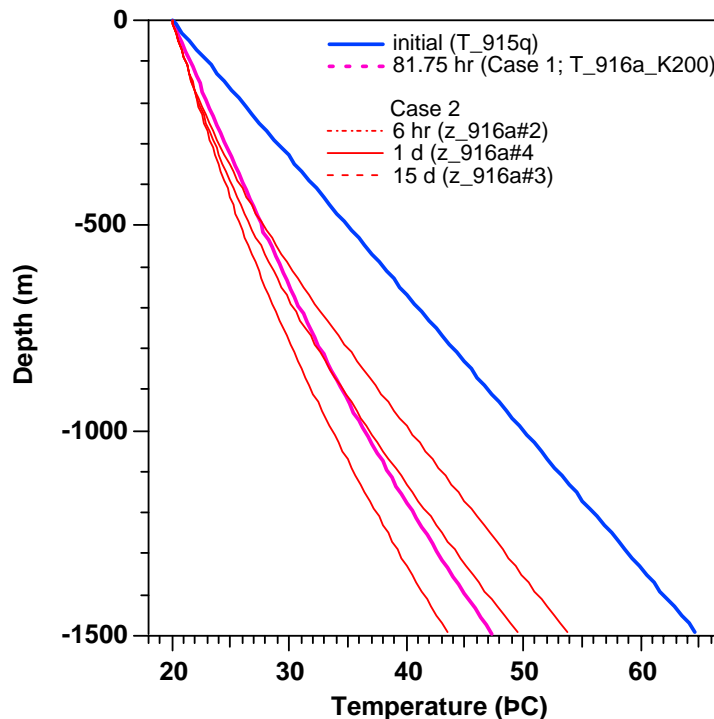

Figure B-4. Simulated temperature profiles in a flowing CO_2 injection well at different times. The initial geothermal gradient is also shown.
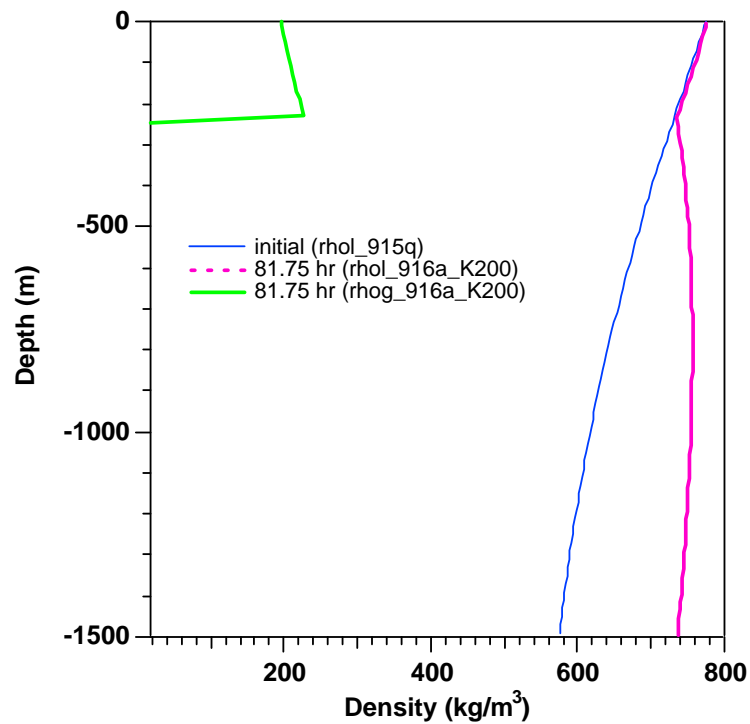
Figure B-5. CO_2 density profile in the wellbore after 81.75 hours of injection for Case 1

Figures B-6 and B-7 present T, P-profiles for Cases 1 and 2, respectively. In Case 1, the top portion of the wellbore is in two-phase conditions and plots on the CO_2 saturation line. In Case 2, the CO_2 is in a single-phase liquid condition throughout.
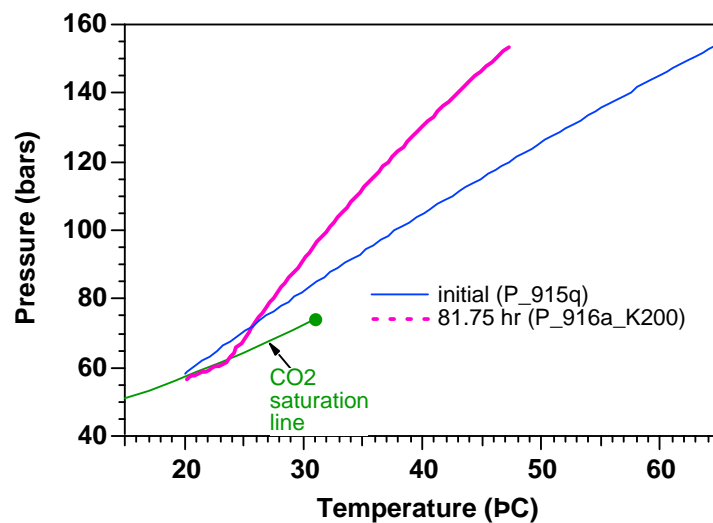

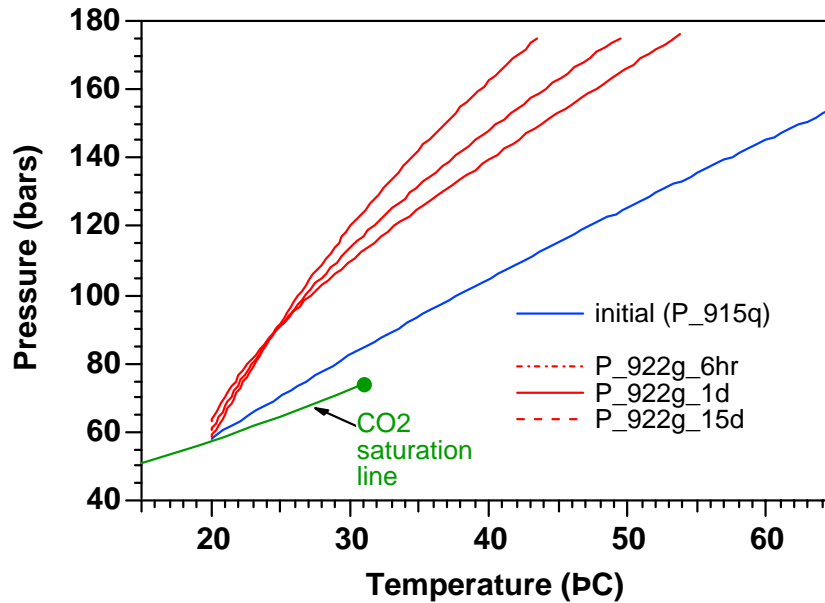**Figure B-6.** Simulated wellbore T, P-profiles in Case 1

Figure B-7. Simulated wellbore T, P-profiles in Case 2

Figure B-8 gives simulated P, T conditions at the sandface for Case 2. Sandface temperatures generally decline as cooler fluids are flowing down the wellbore. The CO_2 reaches the sandface and begins to flow out into the formation at approximately 10^4 s, at which time there is a significant transient increase in temperature, owing to heat of dissolution effects as the CO_2 partially dissolves in formation water.
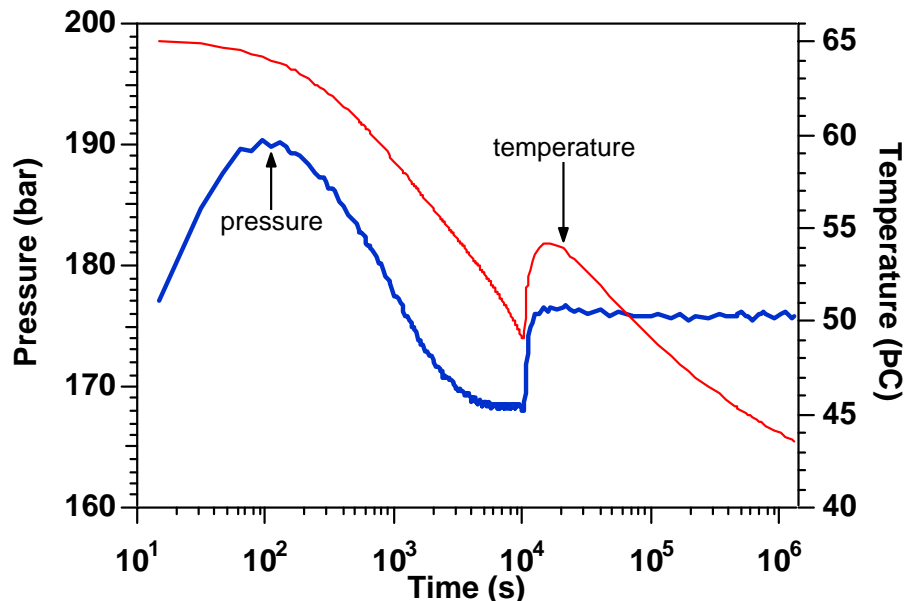

Figure B-8. Simulated sandface conditions of pressure and temperature for Case 2

Downhole pressure evolution reflects a complex superposition of wellbore, temperature, and multiphase flow effects. Pressure response is very different from what would be obtained if a step change in CO_2 rate at the sandface could be imposed. The complex pressure response seen in our simulations suggests that interpretation of pressure transients, whether at the injection well or at a monitoring well at some distance, will not be an easy task.

References

Carroll, J.J., and D.W. Lui, Density, phase behavior keys to acid gas injection. Oil & Gas J., **95** (25), pp. 63–72, 1997.

Stone, H.L., Probability model for estimating three-phase relative permeability. Trans. SPE of AIME, **249**, pp. 214–218, 1970.